NASA CR-72132
GA-7473

(Title unclassified)

STUDIES OF THERMIONIC MATERIALS FOR SPACE POWER APPLICATIONS

Quarterly Progress Report for the Period
June 1, 1966 through August 31, 1966

by

Members of the Direct Conversion Project

Sponsored by
National Aeronautics and Space Administration
Lewis Research Center

GENERAL ATOMIC
DIVISION OF
GENERAL DYNAMICS
JOHN JAY HOPKINS LABORATORY FOR PURE AND APPLIED SCIENCE
P.O. BOX 608, SAN DIEGO, CALIFORNIA 92112

Contract NAS 3-6471
Issued: December 20, 1966

N13-70348
NASA CR-72132
GA-7473
Copy No.

(Title unclassified)

STUDIES OF THERMIONIC MATERIALS FOR SPACE POWER APPLICATIONS

Quarterly Progress Report for the Period
June 1, 1966 through August 31, 1966

by

Members of the Direct Conversion Project

Sponsored by
National Aeronautics and Space Administration
Lewis Research Center

Technical Management
NASA-Lewis Research Center
Nuclear Power Technology Branch
J. W. R. Creagh

During the period of this report, the following "reportable items" as defined by the article "Report of New Technology" evolved: None.

GENERAL ATOMIC
DIVISION OF
GENERAL DYNAMICS

JOHN JAY HOPKINS LABORATORY FOR PURE AND APPLIED SCIENCE

P.O. BOX 608, SAN DIEGO, CALIFORNIA 92112

Contract: NAS 3-6471 Issued: December 20, 1966

NOTICE

This report was prepared as an account of Government-sponsored work. Neithe the United States, nor the National Aeronautics and Space Administration (NASA), nor any person acting on behalf of NASA:

A.) Makes any warranty or representation, expressed or implied, with respect to the accuracy, completeness, or usefulness of the information contained in this report, or that the use of any information, apparatus, method, or process disclosed in this report may not infringe privately owned rights: or

B.) Assumes any liabilities with respect to the use of, or for damages resulting from the use of, any information, apparatus, method or process disclosed in this report.

As used above, "person acting on behalf of NASA" includes any employee or contractor of NASA, or employee of such contractor, to the extent that such employee or contractor of NASA, or employee of such contractor, prepares, disseminates, or provides access to, any information pursuant to his employment or contract with NASA, or his employment with such contractor.

Requests for copies of this report should be referred to

National Aeronautics and Space Administration
Office of Scientific and Technical Information
Attention: AFSS-A
Washington, D. C. 20546

PREVIOUS REPORTS IN THIS SERIES

NASA CR-54958--Quarterly Progress Report for the Period November 23, 1965 through February 28, 1966 (GA-7070)

NASA CR-72032--Quarterly Progress Report for the Period March 1, 1966 through May 31, 1966, (GA-7250)

DIRECT CONVERSION PROJECT MANAGER R. W. Pidd

PRINCIPAL INVESTIGATOR Contract NAS 3-6471 L. Yang

Work done by

Members of the Direct Conversion Project

This page is intentionally blank.

INTRODUCTION

This report describes the work carried out under Contract NAS 3-6471 during the period June 1, 1966 to August 31, 1966 for the development of materials for nuclear thermionic space power applications. Previous work under this contract has been described in the Summary Report for the period September 1, 1964 to November 22, 1965[1], the quarterly report for the period November 23, 1965 to February 28, 1966[2], and the quarterly report for the period March 1, 1966 to May 31, 1966[3]. During this quarter period, the two subjects included under Contract NAS 3-6471 are:

1. Fabrication of cesiated converters LC-6, 7, 8 and 9.
2. Irradiation studies of thermionic materials.

Studies of other subjects of nuclear thermionic interest are being pursued concurrently with these two subjects under Contract NAS 3-8504.

This page is intentionally blank.

CONTENTS

PART I. CONVERTER FABRICATION

(H. Horner)

1.1. COMPONENT FABRICATION

1.1.1. Emitter

LC-7 Emitter

Outgassing of the first 0.010 inch thick deposition of the stem at 2000°C for 50 hours was completed. The pressure in the outgassing station was maintained at 5×10^{-8} torr. A second and final stem deposition of vapor deposited tungsten was performed, heat treated at 1800°C for 2 hours and machined to final configuration. Brazing of the tantalum emitter transition piece to the emitter stem was accomplished without incident and the transition piece was machined to final configuration and fit to the filament holder. The emitter was given to test personnel for measurements of vacuum emission and temperature distribution. Degassing of the emitter structure was completed during vacuum emission measurements.

LC-8 Emitter

Cracks developed in the first encapsulation (fuel slot forming layer) of vapor deposited tungsten over the LC-8 emitter blank at fuel slot edges. This necessitated redeposition of the fuel slot covering. During heat treating of this deposition, a crack developed in the 0.010 thick stem. The initial layer was removed a second time, new molybdenum fuel slot and stem forming mandrels were again machined and outgassed, and the stem and fuel slot covering were again deposited.

Machining, heat treating and degassing at 2000°C for 50 hours of the LC-8 emitter structure in preparation for fuel loading and sealing were successfully accomplished on the third iteration. Machining of a back-up emitter blank structure and mandrels was initiated.

Fuel slabs, fabricated last quarter, were found to be slightly hypostoichiometric in carbon. The order of converter fabrication was therefore changed, with LC-9 scheduled to be completed prior to LC-8. This allows refabrication of the LC-8 fuel to ensure its carbon content to be hyperstoichiometric. Fuel refabrication was initiated during August.

LC-9 Emitter

In June, the first stem deposition, outgassed at 2000°C for 50 hours, was contaminated at San Fernando Laboratories during plating of the second stem deposition and as a result, the plating was removed. The stem fabrication and outgassing sequence was re-initiated and successfully carried through to the completion of the second stem forming deposit.

In parallel to the above work, experimental work was being performed to determine if a high work function tungsten layer (deposited using tungsten hexachloride as the plating gas instead of tungsten hexafluoride) having {110} instead of {100} orientation, could be deposited onto the LC-9 emitter to yield a high performance emitter. A cylindrical geometry chloride-fluoride tungsten duplex test specimen was fabricated for physical and mechanical evaluation. Grinding studies after an 1800°C stress relief indicated that there would be no problem in machining the duplex structure. Samples of the structure were heat treated at 2000°C and 2200°C and then evaluated by metallography and by X-ray diffraction studies. X-ray diffraction results indicated no preferred crystal orientation. Metallography of the heat treated specimens revealed that the chloride tungsten structure was completely recrystallized and that a layer of porosity had developed near the chloride-fluoride interface. The structure is shown in Fig. 1.1.

It was decided that the LC-9 emitter structure should be plated with chloride tungsten and subjected to X-ray diffraction orientation studies and vacuum emission measurements. It was felt that if the coating was completely random or exhibited a poor vacuum work function, the coating could be easily removed and replaced with an emitter surface deposited with tungsten from the hexafluoride.

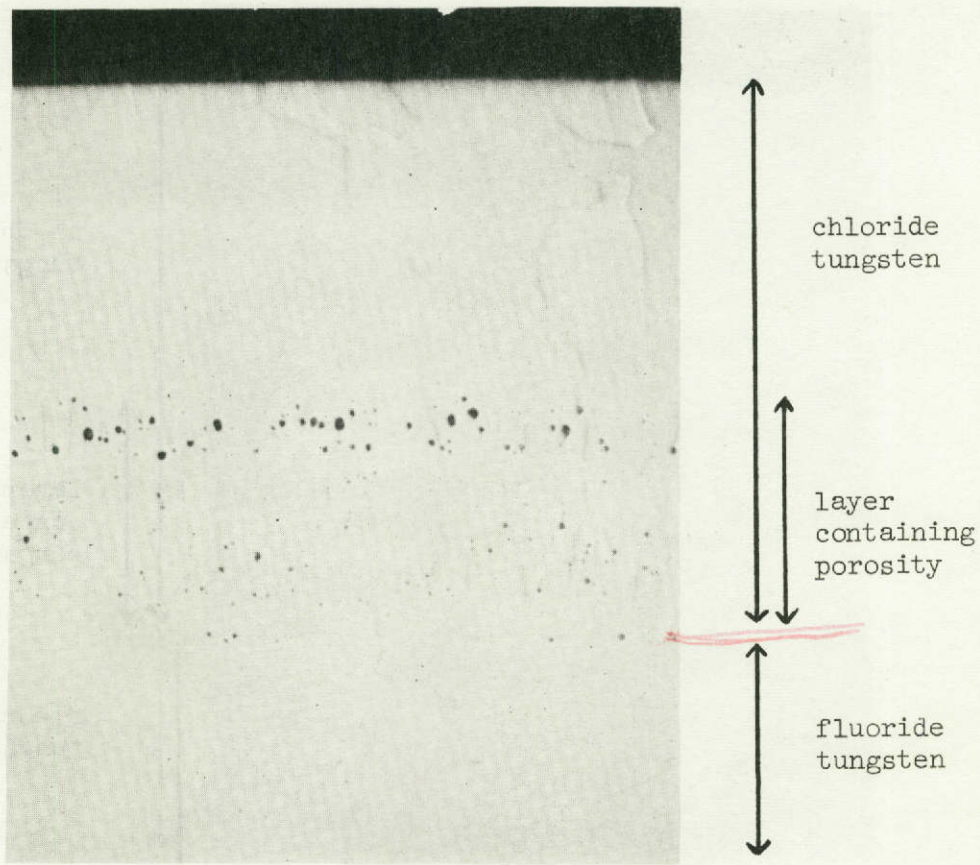

M 16987-3 X200

(a) Unetched

Fig. 1.1(a)--Duplex fluoride-chloride tungsten emitter sample structure after 2200°C heat treatment

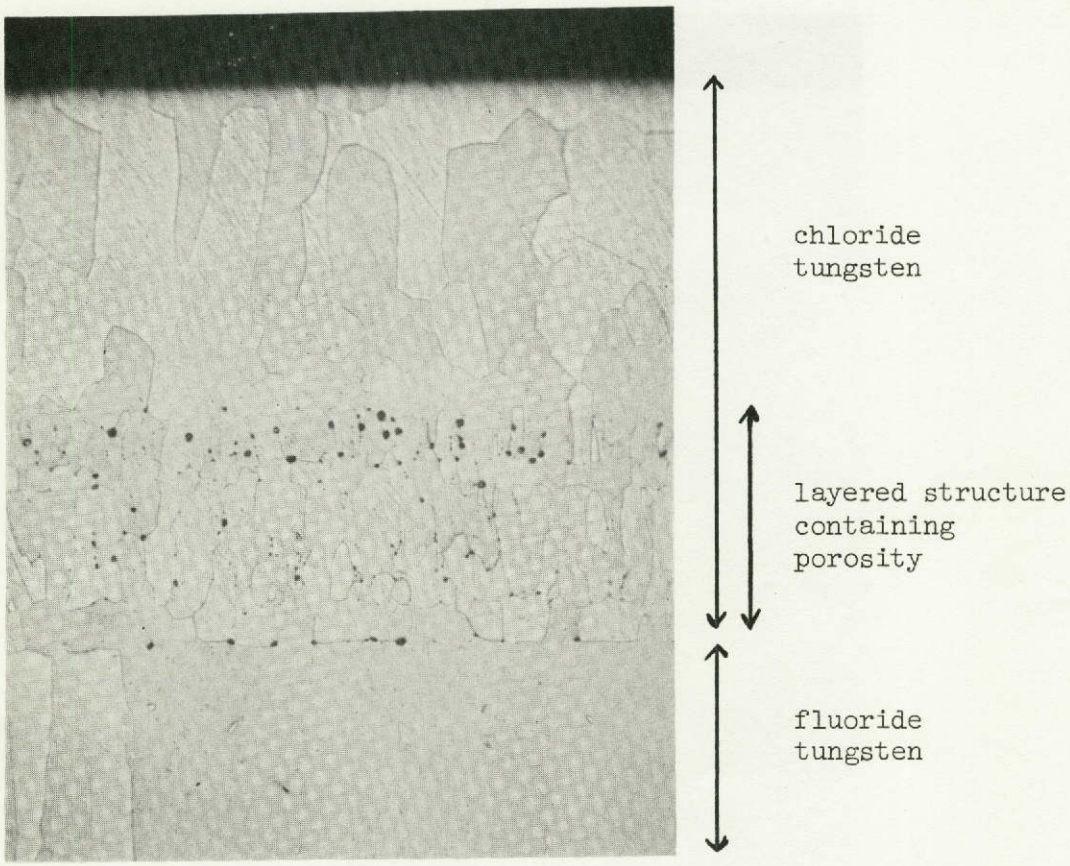

M 16987-4 X200

(b) Etched

Fig. 1.1(b)--Duplex fluoride-chloride tungsten emitter sample structure after 2200°C heat treatment

Note that porosity has developed in the portion of the chloride tungsten structure that shows layering as if the deposition had been interrupted and re-initiated several times. Note also that the fluoride tungsten has retained its columnar structure

Emitter construction was completed by machining the fluoride tungsten emitter substrate to proper size to accept an outer layer of chloride tungsten. The coating was performed and initial heat treating at 1800°C and finish machining were accomplished. Evaluation of the emitter structure will be carried out in September.

1.1.2. Envelope Components

Outgassing of the emitter transition pieces, the collectors and the cesium lead tubes was completed for all three cells, LC-7, 8 and 9, at 1800°C by electron bombardment. Component temperatures were monitored, using tungsten-rhenium thermocouples. The chamber pressure and constitution were monitored with a Varian Associates Partial Pressure Gauge. A typical gas analysis (taken during outgassing of the collectors) is shown below:

RESIDUAL GAS ANALYSES OF CHAMBER WITH Nb COLLECTORS AT 1800°C AFTER 4 HRS.

Gas	Partial Pressure (torr)
H_2	2.39×10^{-7}
CH_4	6.07×10^{-9}
H_2O	5.46×10^{-8}
CO, N_2	1.4×10^{-7}
Ar	2.79×10^{-8}
CO_2	1.99×10^{-8}

Degassing was limited to a 2-4 hour period, as provided by NASA Technical Direction.

Components for the copper cesium reservoir were outgassed at 700°C for 50 hours at 10^{-7} torr. residual gas pressure.

1.1.3. Heat Sink Fabrication

Tantalum sheathed heater wires were brazed to the LC-7, 8 and 9 collector heat sink niobium blanks. A shorted condition during one braze

caused the heaters on the LC-8 sink to be ruined. Replacement has been initiated. The LC-7 heat sink was shrink-fitted and copper brazed to a stainless steel ring (inner half of the cooling gas annulus), machined for assembly welding and welded to the water-cooled stainless steel ring which forms the outer half of the gas annulus. The current lead was then attached The LC-9 collector heat sink was carried to the point of welding to the water-cooled stainless steel ring. Figure 1.2 shows the LC-7 heat sink.

1.1.4. Filament Holder Assembly

Components for all three filament holder assemblies were machined and assembly brazing for the assemblies was completed. Filaments were fabricated for LC-7 and LC-9 holders. The completion of the LC-7 filament and holder was coincident with the completion of the emitter so that final degassing and vacuum emission measurements could be accomplished.

1.2. LC-7 ASSEMBLY

The insulator was welded to the emitter structure. After machining the lower insulator skirt to alignment with the emitter, the collector was fit to the insulator and lapped to the collector heat sink. Figure 1.3 shows the converter components.

The collector was welded to the cesium lead tube to complete the collector sub-assembly.

The emitter and collector sub-assemblies were set up for final outgassing and remote assembly. The setup included a Varian partial pressure gauge for residual gas analyses during degassing of the assembled cell.

Outgassing and final assembly brazing proceeded without incident. High temperature emitter-outgassing for LC-7 was conducted after final assembly was complete. The cell closure braze was leak tight and the cell was given to test group personnel for final outgassing.

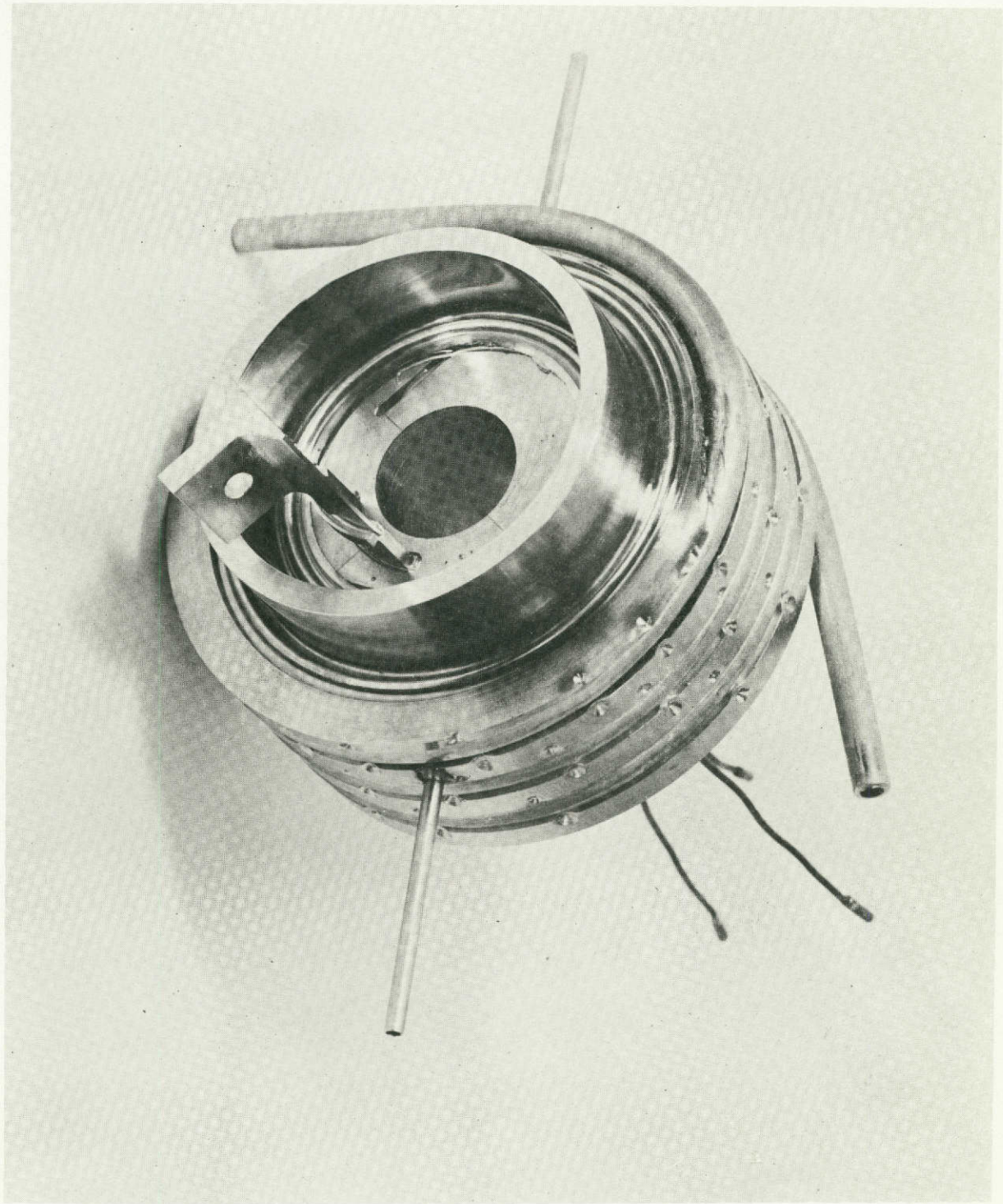

TE 46245

~ .8X

Fig. 1.2--LC-7 collector heat sink

DC-359

(a) LC-7 emitter structure

Fig. 1.3(a)--LC-7 Emitter and collector structures before assembly

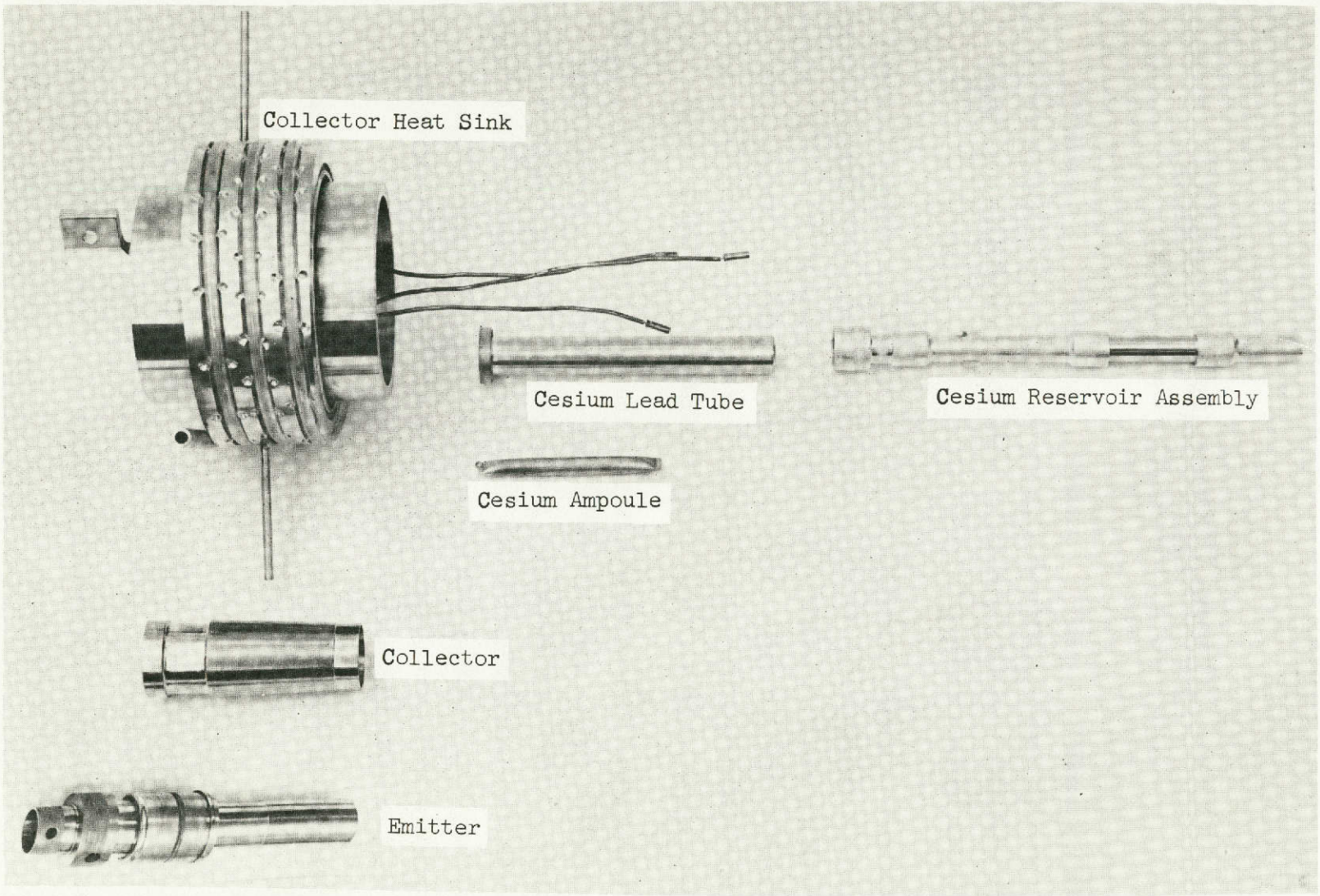

DC-362-5

(b) All cell components

Fig. 1.3(b)--LC-7 Components before assembly

PART II. IRRADIATION STUDY OF THERMIONIC MATERIALS

(J. Sleigh, A. Steeger, J. Ream, W. Godsin)

Two meetings were held at NASA-Lewis during this period, which covered the performance of Capsules 213-1 and 213-2, the problems encountered with the capsule positioning mechanism, and the capsule and carriage redesign approaches.

Parametric thermal analysis of the relationships between fuel and thermal bond temperatures, fission power density, and other parameters were completed using the G.A. radial-axial heat transfer code "RAT". The details are included in the Appendix. There was general agreement between the fission power density, thermal bond temperatures, fuel temperatures, and the results of the nuclear analysis for the location in the V-2 tube.

It was believed desirable to retain the capsule-positioning mechanism cylinder concept but to modify it by adding shaft seals and using hard chrome plate against 17-4 PH on all moving parts. Several conceptual designs of a new carriage were presented for discussion and evaluation. Utilizing two stationary ball bushings and a single carriage shaft driven directly by the cylinder shaft was the most favorable approach. A layout of this concept will be made and submitted for NASA approval.

A conceptual design of the next irradiation capsules based on the following ground rules previously agreed upon was also presented and accepted.

1. The design goal of fuel temperature accuracy is $\pm 50^{\circ}C$ but a fuel temperature accuracy of $\pm 100^{\circ}C$ is acceptable.
2. Fuel temperature should be calculable from low temperature thermocouple readings.
3. Total heat generation rate and fission power should be determinable from calorimetric measurement.

4. A γ-heating monitor should be incorporated in the capsule.

5. Inconel confinement can of high and stable thermal emissivity should be used.

6. Thermal shields for fuel samples should be retained in order to minimize axial temperature gradient in the fuel samples.

7. Fuel sample dimensions as close as possible to that in a thermionic fuel element should be employed.

Thermal and nuclear calculations will be completed to establish the various parameters. A mock-up capsule will be irradiated for one cycle prior to capsule installing V-2C and V-2D to determine gamma heat values and hopefully optimum axial position.

REFERENCES

1. "Studies of Thermionic Materials for Space Power Applications, Summary Report, September 1, 1964 through November 23, 1965" (U), National Aeronautics and Space Administration Report NASA CR-54980. General Atomic Division, General Dynamics Corporation, May 6, 1966. C/RD

2. "Studies of Thermionic Materials for Space Power Applications, Quarterly Progress Report for the Period November 23, 1965 through February 28, 1966" (U), National Aeronautics and Space Administration Report NASA CR-54966. General Atomic Division, General Dynamics Corporation, June 10, 1966. (C/RD)

3. "Studies of Thermionic Materials for Space Power Applications, Quarterly Progress Report for the Period March 1, 1966 through May 31, 1966" (U), National Aeronautics and Space Administration Report NASA CR-72043. General Atomic Division, General Dynamics Corporation, September 21, 1966. (C/RD)

APPENDIX

EVALUATION OF THE THERMAL PERFORMANCE OF THERMIONIC MATERIALS CAPSULES 213-1 AND 213-2 IN PLUM BROOK REACTOR

Contents

SUMMARY

Parametric thermal analyses have been performed for Capsules 213-1 and 213-2 which were irradiated side by side in the V-2 tube position in Plum Brook Reactor Facility for two reactor cycles. The relationships among fuel temperature, thermal bond temperature, fission power density and other operating variables were established by use of the General Atomic radial-axial heat transfer code "RAT". The range of fission power density deduced from the observed thermal bond temperature by thermal analysis is in general agreement with that obtained by nuclear analysis for the capsule location in the V-2 tube. The calculations and measurements of the relationship between the fuel temperature and thermal bond temperature agreed well for fuel pod 213-6 but not for fuel pod 213-3. The fuel temperatures, fission power densities and the uncertainties in these quantities were calculated as a function of time for the four fuel pods. The thermal performance of the fuel pods indicates that each capsule was exposed to equivalent neutron fluxes but that the optimum vertical position of the capsules is about two to four inches higher than the location where the irradiation was performed.

DESCRIPTION OF EXPERIMENT AND SUMMARY OF EXPERIMENT DATA

This experiment (Number 62-13-R1) is concerned with the study in Plum Brook Reactor Facility of the irradiation behaviors of vapor-deposited tungsten clad UC-ZrC and tungsten-cermet fuels for thermionic applications. Two identical capsules, each of which contains two fuel pods, were installed in the V-2 tube facility at similar positions with respect to the reactor core, and irradiated for two reactor cycles (Cycle 42-P and Cycle 43-P). Figure A.1(a) illustrates the cross section of the capsule and Fig. A.1(b) shows schematically the locations and the designations of the fuel pods and thermocouples. Shown in the same figure are also a set of temperature readings of these thermocouples during the initial startup. While all of the low temperature Chromel-Alumel thermocouples (No. 1, 13, 3, 15, 2, 14, 4 and 16) used for the indication of the capsule thermal bond temperatures performed satisfactorily throughout the two reactor cycles, only two high temperature W-Re thermocouples (No. 5 and 8) used for measuring the fuel temperatures recorded reasonable readings (1730°C by T/C No. 8 in fuel pod

Fig. A.1(a)--Capsule Schematic Cross-Section

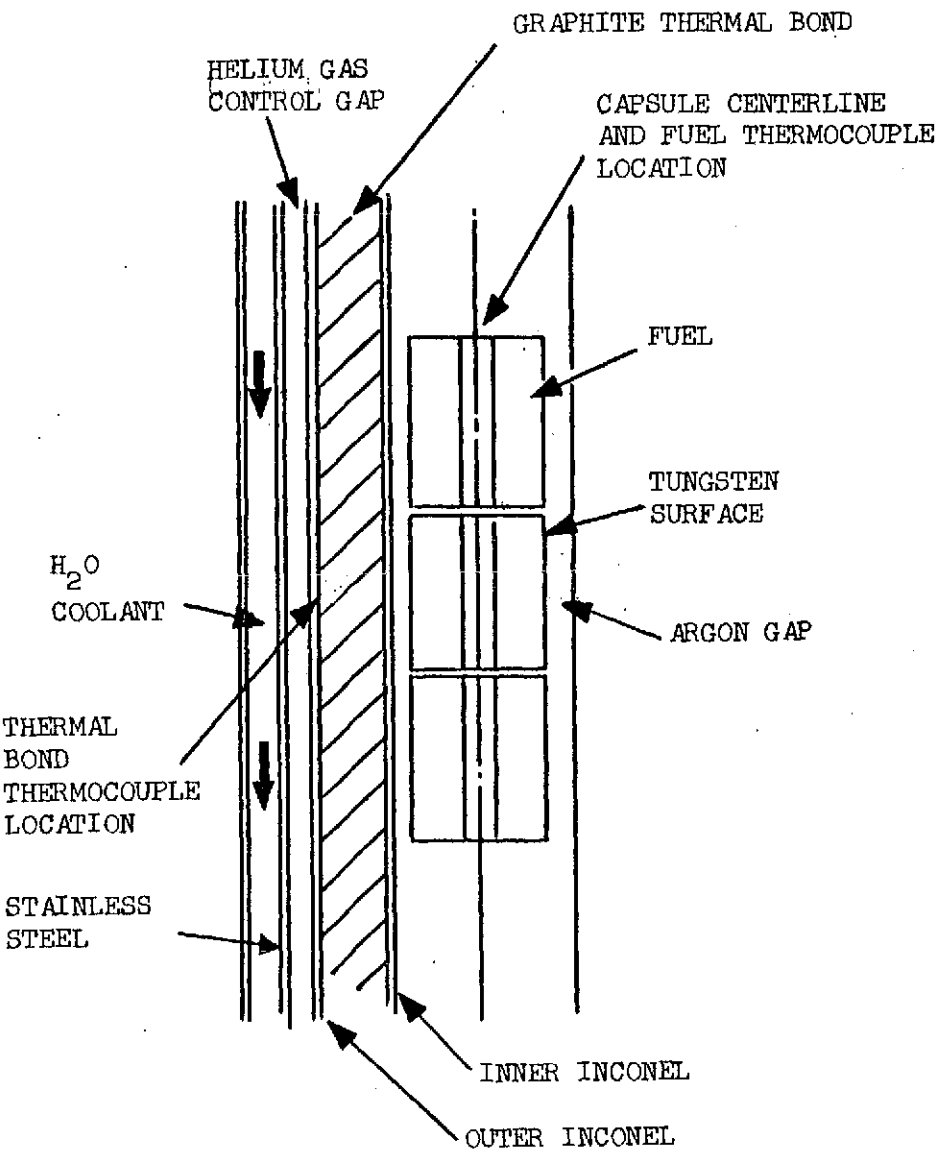

Fig. A.1(b)--Schematic of Fuel Pods and Thermocouple Locations

The temperatures indicated represent thermocouple readings during the initial startup.

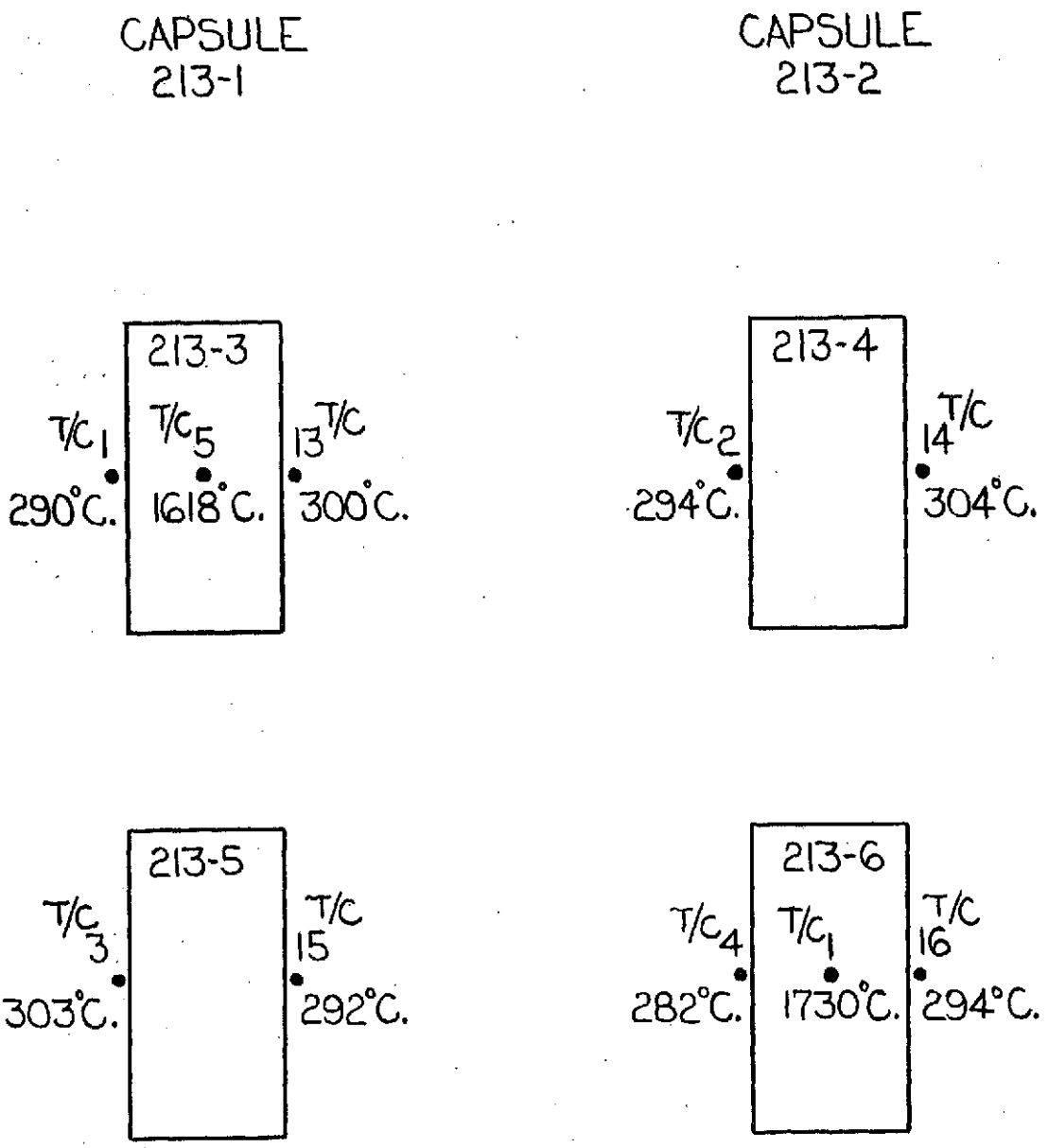

213-6 and 1618°C by T/C No. 5 in fuel pod 213-3). These two thermocouples provided believable readings only during a portion of the first reactor power cycle. Figure A.2 shows the experimentally determined relationship between the readings of the high temperature thermocouple No. 8 and the corresponding average thermal bond temperatures (average of T/C No. 4 and T/C No. 16 readings) of fuel pod 213-6 during the initial startup. Figure A.3 contains the chronological records of the average thermal bond temperature of each of the four fuel pods during the two reactor cycles. The experiment was terminated after the second cycle irradiation because of the malfunction of the capsule-positioning mechanism.

PURPOSE AND PROCEDURES OF PRESENT EVALUATION

The purpose of the present evaluation is to provide a means for estimating the fuel temperatures and the fission power densities prevailing in each of the four irradiated fuel pods as a function of irradiation time. The evaluation was based on the experimental data shown in Figs. A.1, A.2 and A.3.

The procedures adopted consist of the following:

(1) Establish the parameters which determine the relationship between fuel temperature, fission power density and thermal bond temperature.

(2) Estimate the uncertainty limits of the values of these parameters, as set by design tolerances or specifications, or chosen by judgement and experience.

(3) Perform parametric analysis of the relationships among fuel temperature, fission power density, thermal bond temperature by using the "RAT" heat transfer code taking into account these uncertainty limits.

(4) Correlate the experimentally determined fuel temperature versus thermal bond temperature relationships for fuel pods 213-6 and 213-3 (see Figs. A.1 and A.2) with parametric analysis results

Fig. A.2--Observed Relationship Between Fuel Temperature and Average Thermal Bond Temperature for Fuel Pod 213-6 During Initial Start-Up. Data taken at 60 MW on 1-3-66

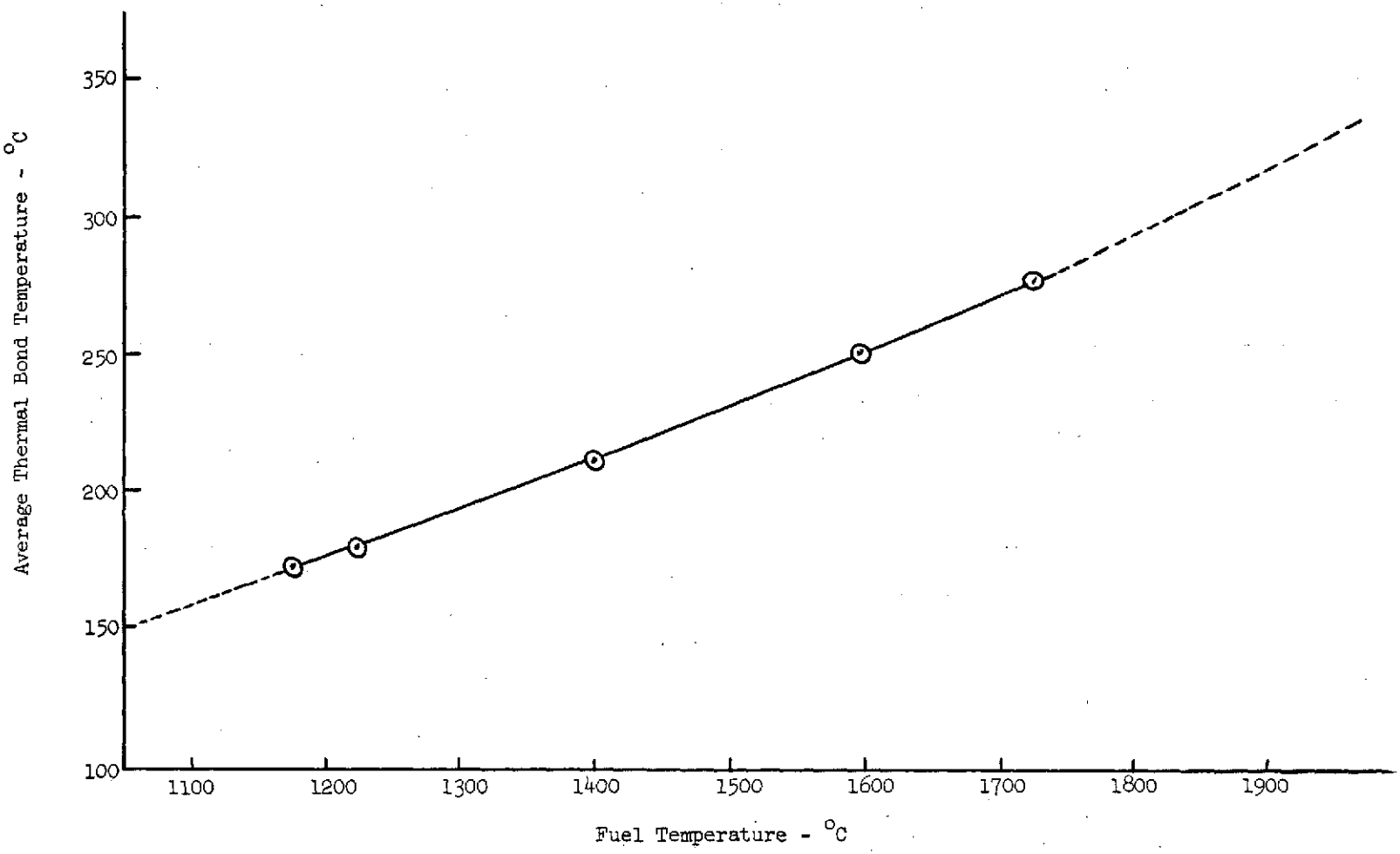

Fig. A.3--Average Thermal Bond Temperatures of the Four Fuel Pods as a Function of Irradiation Time (Corrected for wiring crossover between 213-4 and 213-5)

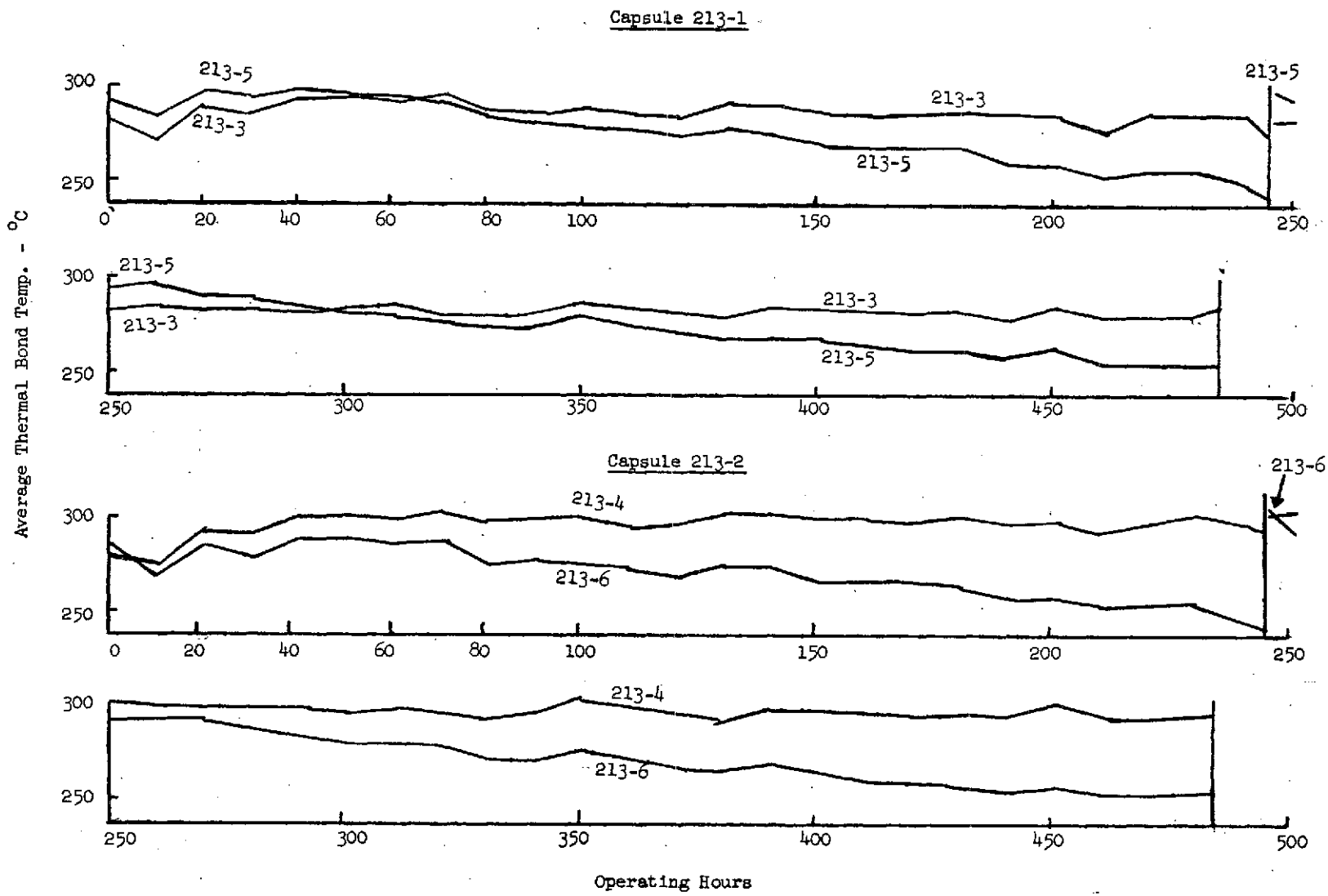

obtained in (3) in order to check the credibility of the observed relationships.

(5) Deduce the fuel temperatures and fission power densities for the four fuel pods as a function of time on the basis of the results obtained in (3) and (4).

SELECTION OF PARAMETERS

For the capsule configuration used (Fig. A.1(a)), the following parameters control the relationship between fuel temperature, fission power density and thermal bond temperature:

(1) Helium gap size
(2) Argon gap size
(3) Total thermal emittance of Inconel
(4) Total thermal emittance of tungsten
(5) γ heating rate
(6) Coolant flow rate
(7) Coolant temperature

DETERMINATION OF UNCERTAINTY LIMITS OF EACH PARAMETER

(1) Helium gap size: 0.017 - 0.019 inch (room temperature), treated as a function of temperature in calculation.

The variation in helium gap size is due to fabrication tolerance.

(2) Argon gap size: 0.0185 inch (room temperature), treated as a function of temperature in calculation.

The diameter of the sample and the diameter of the Inconel are machined and measured to achieve the argon gap; therefore there is no uncertainty in this room temperature gap size. The thermal conductivity data of argon are shown in Fig. A.4. The data from Ref. 2 are the most recent and were used in the calculation.

Fig. A.4--Thermal Conductivity of Argon

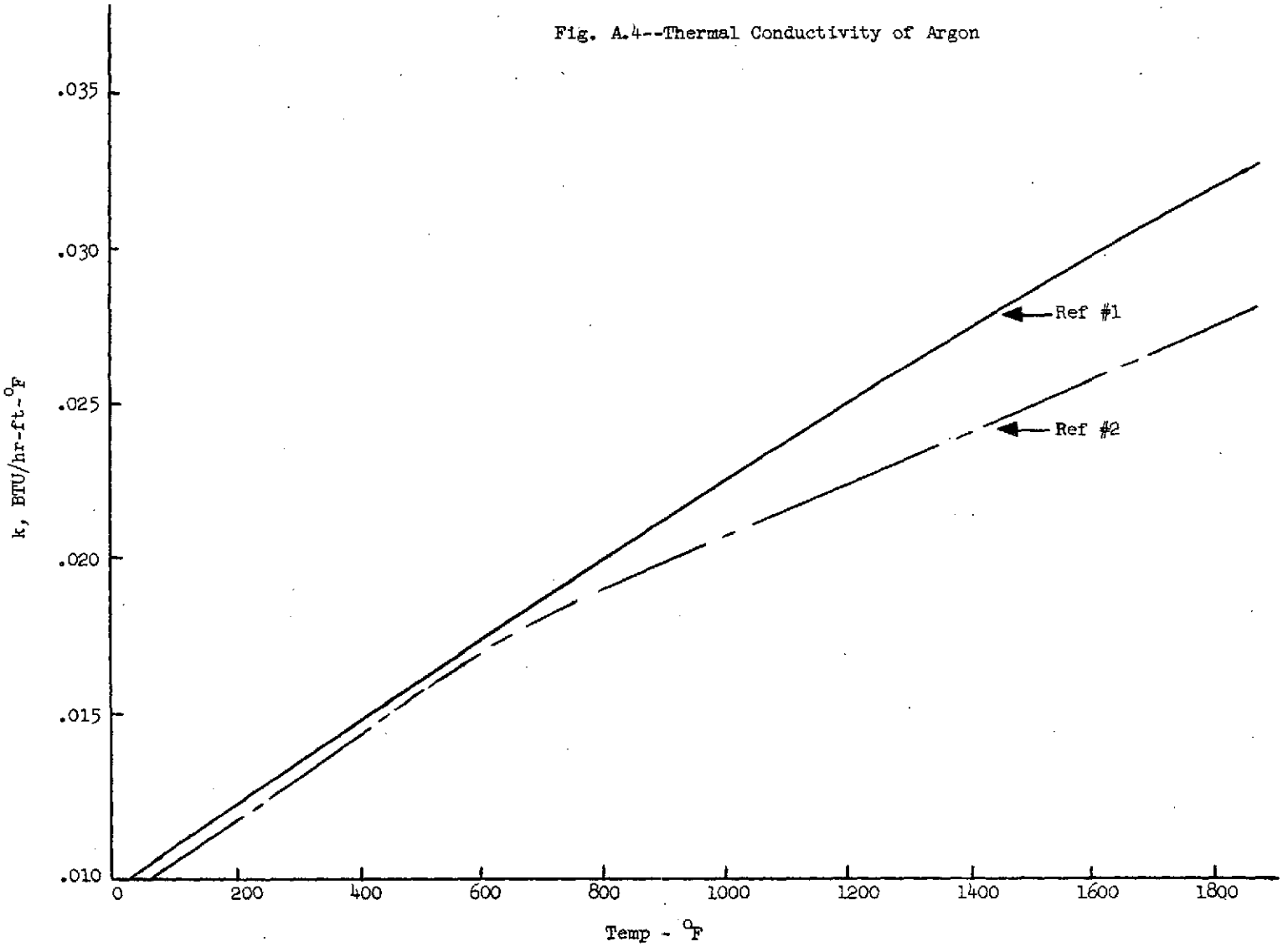

(3) Inconel emittance: 0.15

The capsule drawing (373-SK-57) specifies a 16 micro-inch finish on the Inconel primary containment can, which is a polished surface. For small diameter tubing, honing is the usual process by which close dimensional control and a low surface roughness may be obtained. Handbook values for the emittance of polished Inconel vary somewhat as a function of temperature but show negligible differences in the temperature region of interest (see Fig. A.5). The value is $\sim$ 0.15 at $\sim$ 300°C from either Ref. (3) or Ref. (4) but in actual manipulation of the RAT code (see below) the emittance curve from Ref. (3) may be inserted as an equation with temperature dependence.

(4) Tungsten emittance: 0.26

The value of 0.26 for the emittance of tungsten was selected on the basis of both handbook data (see Fig. A.6) and measurements made at General Atomic on emitter structures. The selected handbook values (Ref. 5) and the measured data agree quite well. The tungsten emittance may also be treated as a function of temperature in code usage.

(5) γ heating rate: 0.5 - 1.0 w/gr

This is consistent with the range of interest in the V-2 tube region.

(6) Coolant flow rate: 4 - 7 GPM

This covers the range measured during the experiment.

(7) Coolant temperature: 125 - 135°F

These represent the temperature of the reactor inlet water and the temperature of the reactor outlet water.

Fig. A.5--Emittance of Polished Inconel

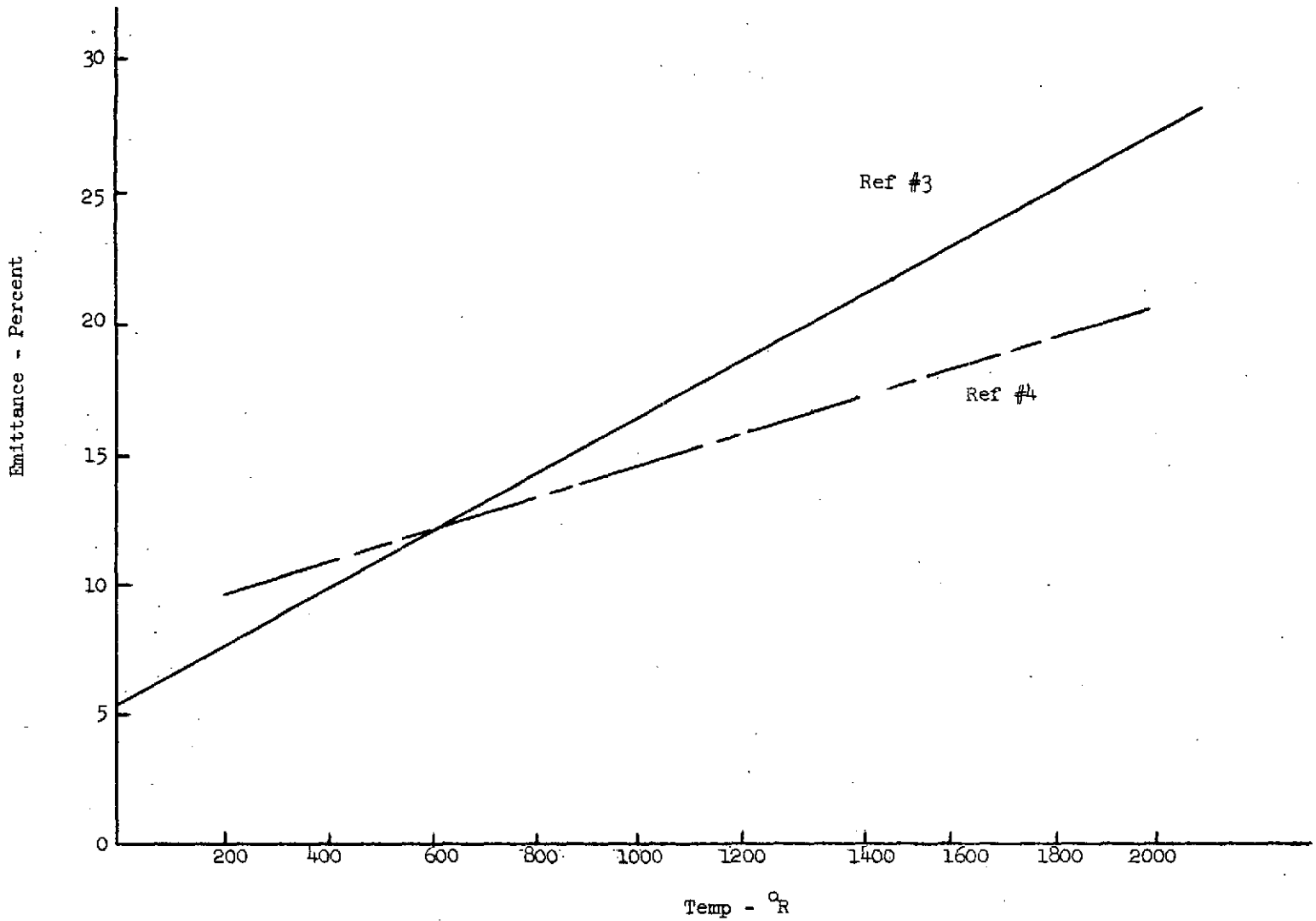

Fig. A.6--Emittance of Polished Tungsten

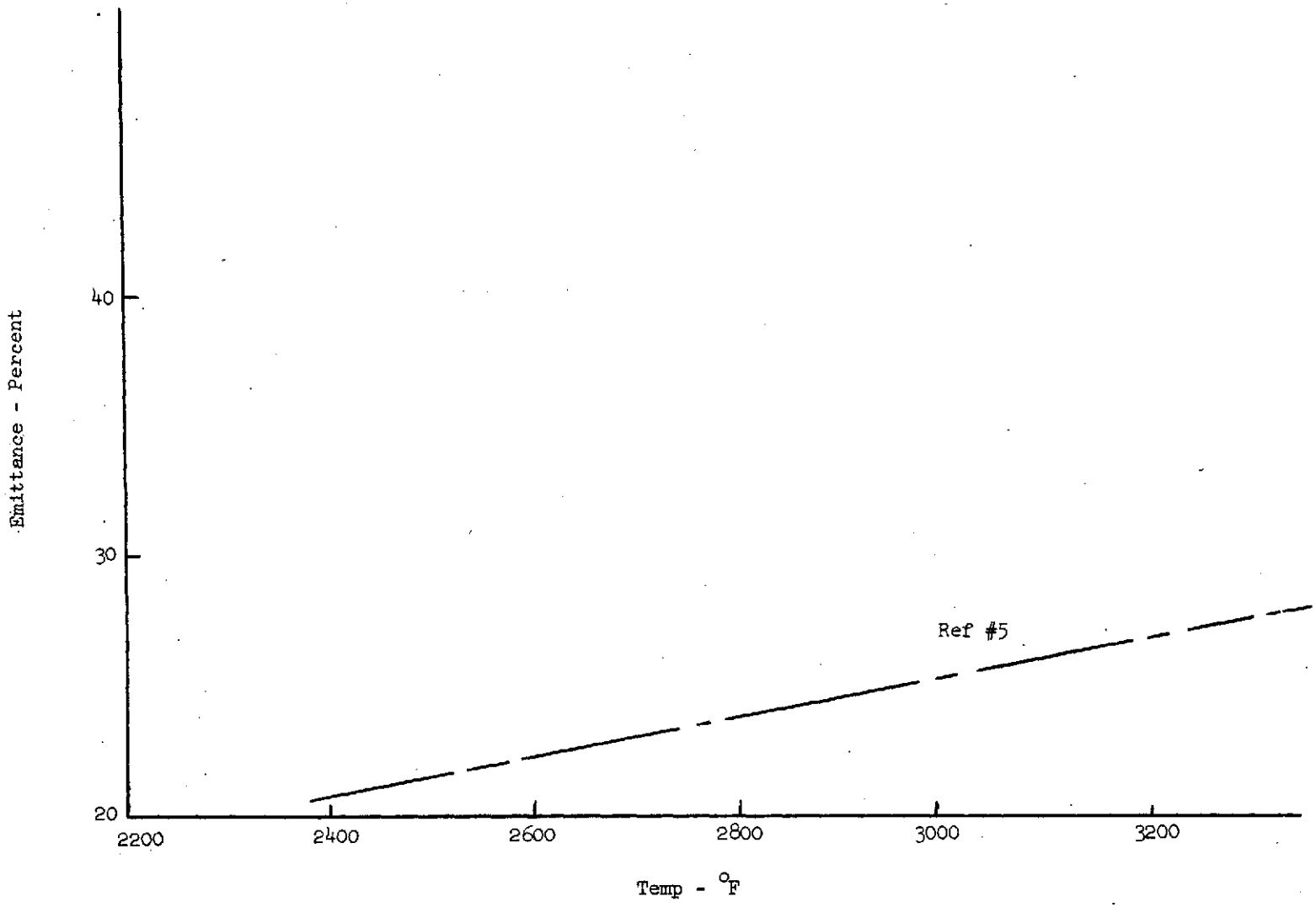

PARAMETRIC ANALYSIS

The radial-axial heat transfer code, "RAT", was used to conduct the analysis. Figure A.7 shows the fuel temperature-thermal bond temperature relationship obtained as a function of γ heating rate, fission power density, helium gap size, coolant flow rate and coolant temperature, with the Inconel emittance, the tungsten emittance and the argon gap size maintained constant. Using these curves, one can deduce the uncertainty limits of fuel temperature and fission power density from the observed thermal bond temperature if the values of these parameters vary in the ranges indicated in the figure. Table A.I shows the changes in the fuel temperature and the thermal bond temperature when each of the parameters shown varies independently from its base value by the indicated amount, with the other parameters staying constant. It can be seen from Table A.I that the size of the helium gap and the γ heating rate are influential in changing the thermal bond temperature, (and fission power density values deduced therefrom) while the fuel temperature is strongly dependent upon the Inconel emittance and the fission power density.

CORRELATION BETWEEN ANALYTICAL AND EXPERIMENTAL RESULTS

Fuel pod 213-6 exhibited the fuel temperature-thermal bond temperature relationship shown in Fig. A.2 during the initial startup. At an average thermal bond temperature of 288°C, the observed fuel temperature was 1730°C. One of the data points for fuel pod 213-3 which contains the other functioning high temperature thermocouple showed a fuel temperature of 1618°C at an average thermal bond temperature of 295°C. In order to ascertain which of the two "fuel temperature-thermal bond temperature" relationships is the more probable one and whether it could be used for establishing the fuel temperature and the fission power density in all the four fuel pods during their two cycle irradiation, comparisons were made between these experimental results and the analytical data. Using Fig. A.7, the calculated maximum and minimum fuel temperature for conditions I and II at gamma heating rates of 0.5 and 1.0 w/gm respectively were determined for thermal bond temperatures of 288°C and 295°C. These values are compared with the observed fuel temperatures in Table A.II. It can be seen that the

Fig. A.7--Parametric Analysis of the Fuel Temperature vs. Thermal Bond Temperature Relationship

Note: In all cases, Inconel emittance* = 0.15, Tungsten emittance* = 0.26, Argon gap size* = 0.0185 inch.

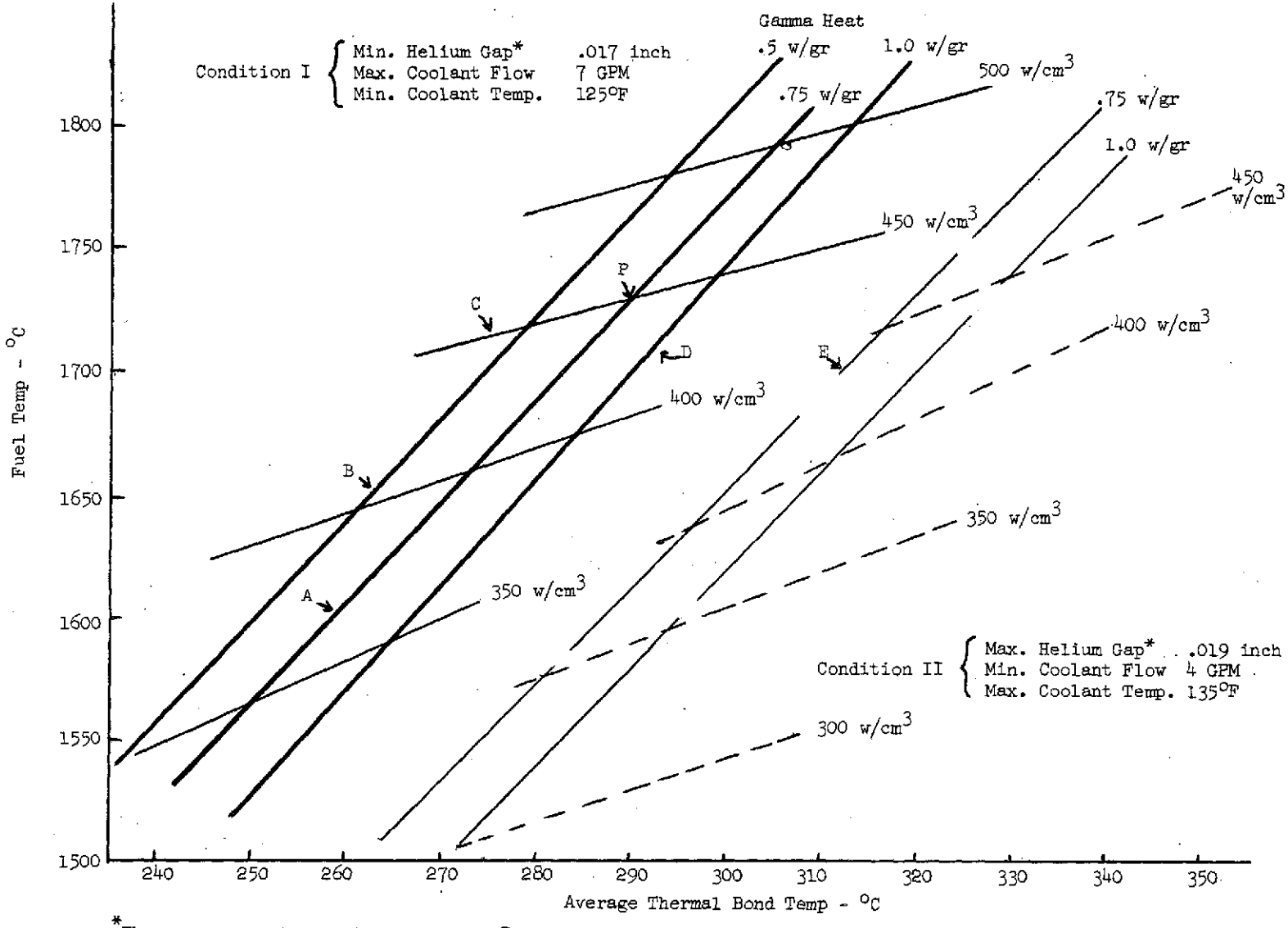

*These are room temperature values. In computation, they are fed in as a function of temperature.

TABLE A.I

Changes in Fuel Temperature and Thermal Bond Temperature with Changes of the Values of Some Parameters

		Variation From Base		Change in Fuel Temp.		Change in Thermal Bond Temp.	
Independent Variables	Base	Amount	%	Degrees Cent.	%	Degrees Cent.	%
Helium Gap	.017"	+.002"	+11%	+3°	0.18%	+20°	8.4%
Argon Gap	.0185"	+.0015"	+8.1%	+32°	+1.9%	0	0
Gamma Heat	.75 w/gr	+.25	+33%	+13°	+0.77%	+10°	4.2%
Fuel Fission Power	440 w/cm3	+110	+25%	+147°	+8.7%	+37°	+15.5%
		-110	-25%	-127°	-7.5%	-40°	-16.8%
Inconel Emittance	≅.15	+.25	+167%	-140°	-8.3%	0	0

Percent change in temperature is based on the temperature above coolant temperature. For the fuel temperature the base was (1730 - 50) = 1680°C, and for the thermal bond the base was (288 - 50) = 238°C.

Tungsten emittance = 0.26

Coolant flow rate = 7 GPM

Coolant temperature = 125°F

TABLE A.II

Comparision of Calculated and Experimental Fuel Temperature in Fuel Pods 213-6 and 213-3

	Thermal Calc.		Experimental Values	
	Pod 213-6	Pod 213-3	Pod 213-6	Pod 213-3
Parameters				
He gap size, inch	.017-.019	.017-.019	--	--
Ar gap size, inch	.0185	.0185	--	--
γ heating rate, w/gr.	0.5-1.0	0.5-1.0	--	--
Inconel emittance	0.15	0.15	--	--
Tungsten emittance	0.26	0.26	--	--
Coolant flow rate GPM	4-7	4-7	6-7	6-7
Coolant temperature ^{o}F	125-135	125-135		
Location in PBR V-2 tube facility	0.2" E of centerline	0.2" E of centerline	0.2" E of centerline	0.2" E of centerline
Thermal bond temperature ^{o}C	288	295	288±.75%*	295±.75%*
Fuel Temperature ^{o}C	1575-1762	1604-1794	1730±1%*	1618±1%*
Fission power density w/cm^3	340-480	360-505	--	--

*Calibration accuracy when thermocouple is functioning

Design Point: He gap size, 017-.019 inch; Ar gap size, .0185 inch; γ heating rate, 1 w/gr; Inconel emittance 0.58; Tungsten emittance, 0.26; Coolant flow rate 5, GPM; Coolant temperature 125, ^{o}F; Location in PBR V-2 tube facility, ~1" E of centerline; Thermal bond temperature 420, ^{o}C; Fuel temperature 1800, ^{o}C; Fission power density 650, w/cm^3.

Nuclear Calc.: γ heating rate, 1 w/gr; Location in PBR V-2 tube facility, 0.2" E of centerline; Fission power density w/cm^3, 350±35%.

observed fuel temperatures in both fuel pods (i.e. 1730°C and 1618°C) fall within the ranges (i.e. 1575-1762°C and 1604-1794°C), of the calculated values. The fission power density obtained from nuclear calculation based on data presented in the Design and Hazards Manual and assuming at γ heating rate of 1 w/gr are also shown. It can be seen that the nuclear calculation data overlaps that of the thermal calculation data.

Although the above comparisons do not lead to a definite conclusion as to whether the fuel temperature - thermal bond temperature relationship in one fuel pod is more credible than that in the other, the following correlation analysis indicates that the relationship established for fuel pod 213-6 during the initial startup is more believable. In Fig. A.8, such an experimentally determined relationship is compared with the calculated ones for the parametric conditions indicated on the figure (which are identical with condition I of Fig. A.7), with the γ heating rate as a variable (0.5, 0.75 and 1.0 w/gr.). It can be seen that the agreement is excellent at a γ heating rate of 0.75 w/gr. In fact, further changes of the parametric conditions within the allowable ranges do not lead to any better agreement. Figure A.9 gives the calculated thermal bond temperature versus fission power density relationship forfuel pod 213-6 for the same parametric conditions as that shown in Fig. A.8. The correlation analysis was therefore believed useful for deducing the fuel temperature and the fission power density from the more reliable thermal bond temperature reading if the capsule operates under the conditions specified in Fig. A.8 and at a γ heating rate of 0.75 w/gr.

Similar comparison between experimental and analytical results was carried out using the previously mentioned data point for fuel pod 213-3 (1618°C fuel temperature versus 295°C average thermal bond temperature). Figures A.10 and A.11 summarize the results obtained. It can be seen that good correlation can be obtained only by assuming a high γ heating rate (1 w/gr.) in conjunction with a low fission power density (350 w/cm^3) for the parametric conditions defined in Fig. A.10, or by assuming a high Inconel emittance (0.40) for the parametric conditions defined in Fig. A.11. From these results it was concluded that the observed temperature relationship during the startup of fuel pod 213-3 (i.e. the 1618°C high temperature

Fig. A.8--Thermal Bond Temperature vs. Fuel Temperature Relationship for Fuel Pod 213-6

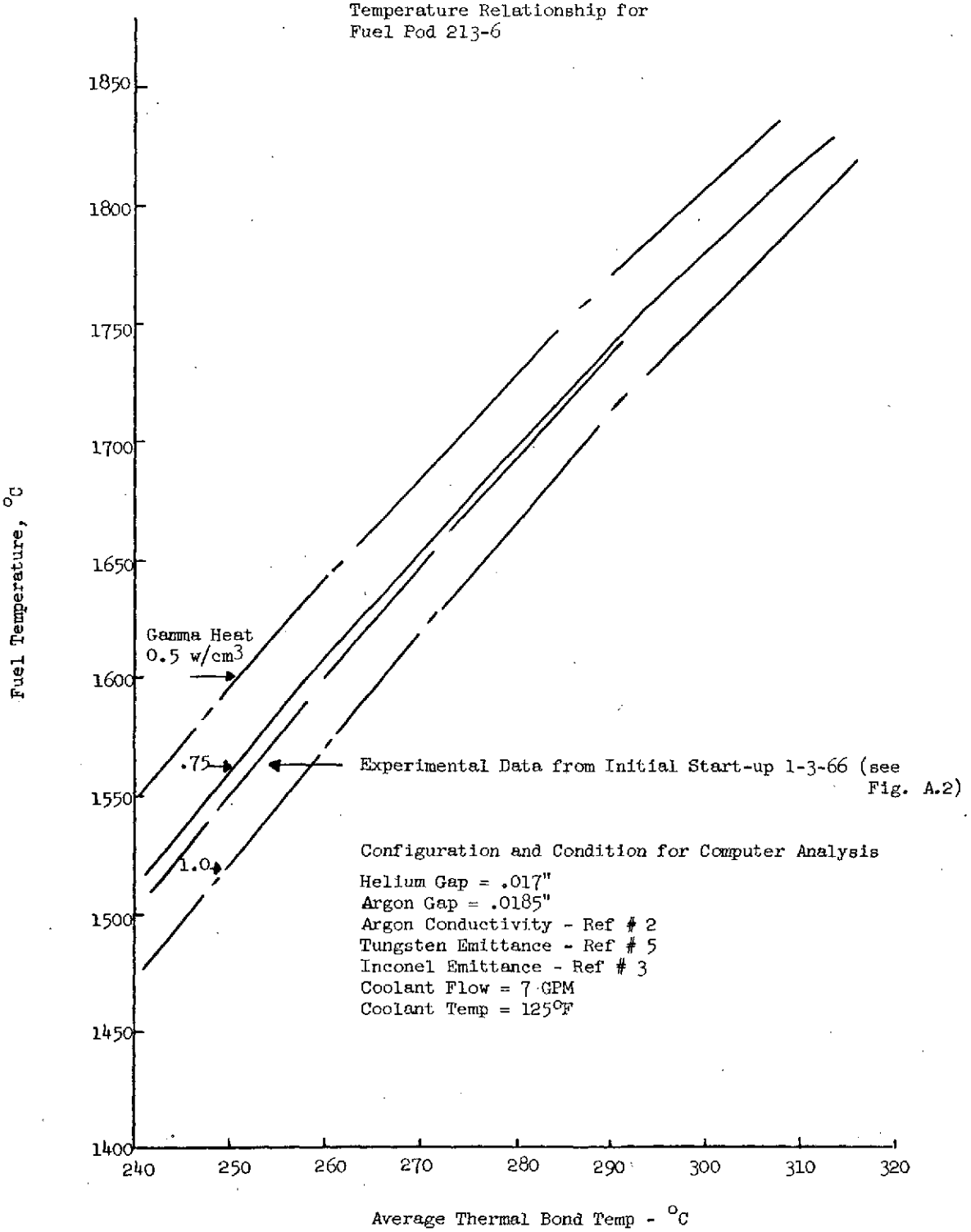

Fig. A.9--Analytical Thermal Bond Temperature vs. Fuel Fission Power Density Relationship for Conditions Specified on Figure A.8

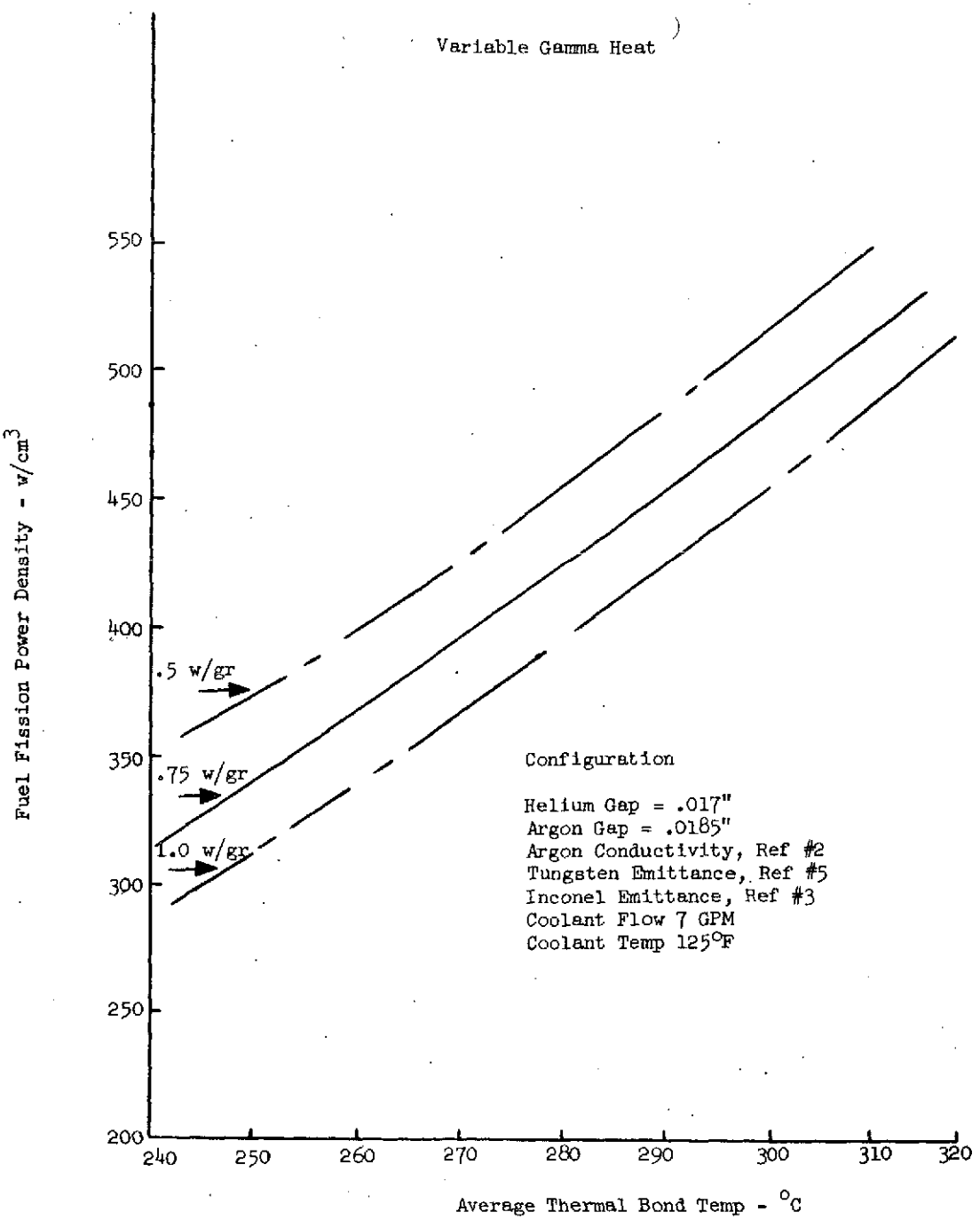

Fig. A.10--Thermal Bond Temperature vs. Fuel Temperature Relationship for Fuel Pod 213-3

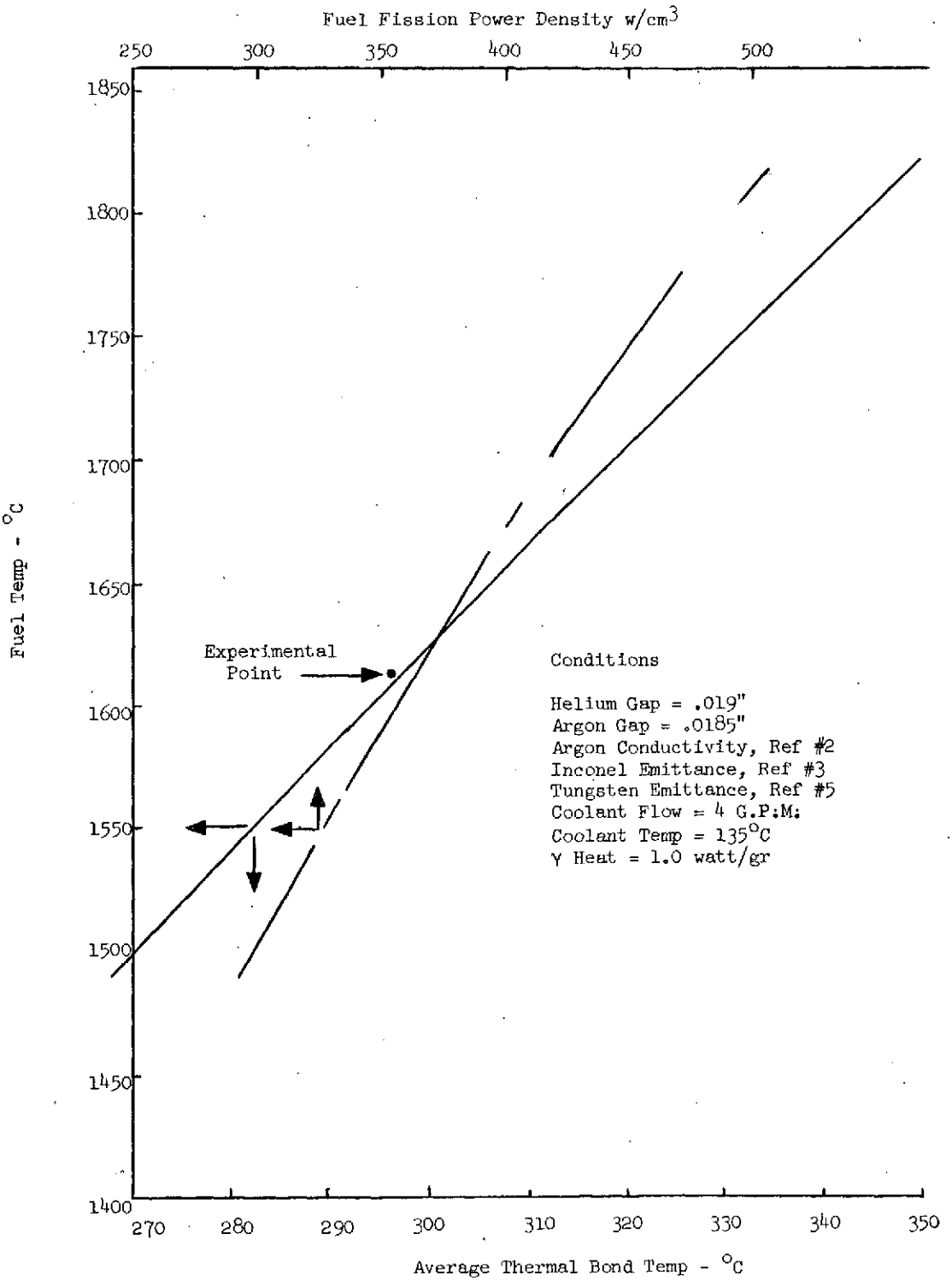

Fig. A.11--Thermal Bond Temperature vs. Fuel Temperature Relationship for Fuel Pod 213-3, with Inconel Emittance as Variable

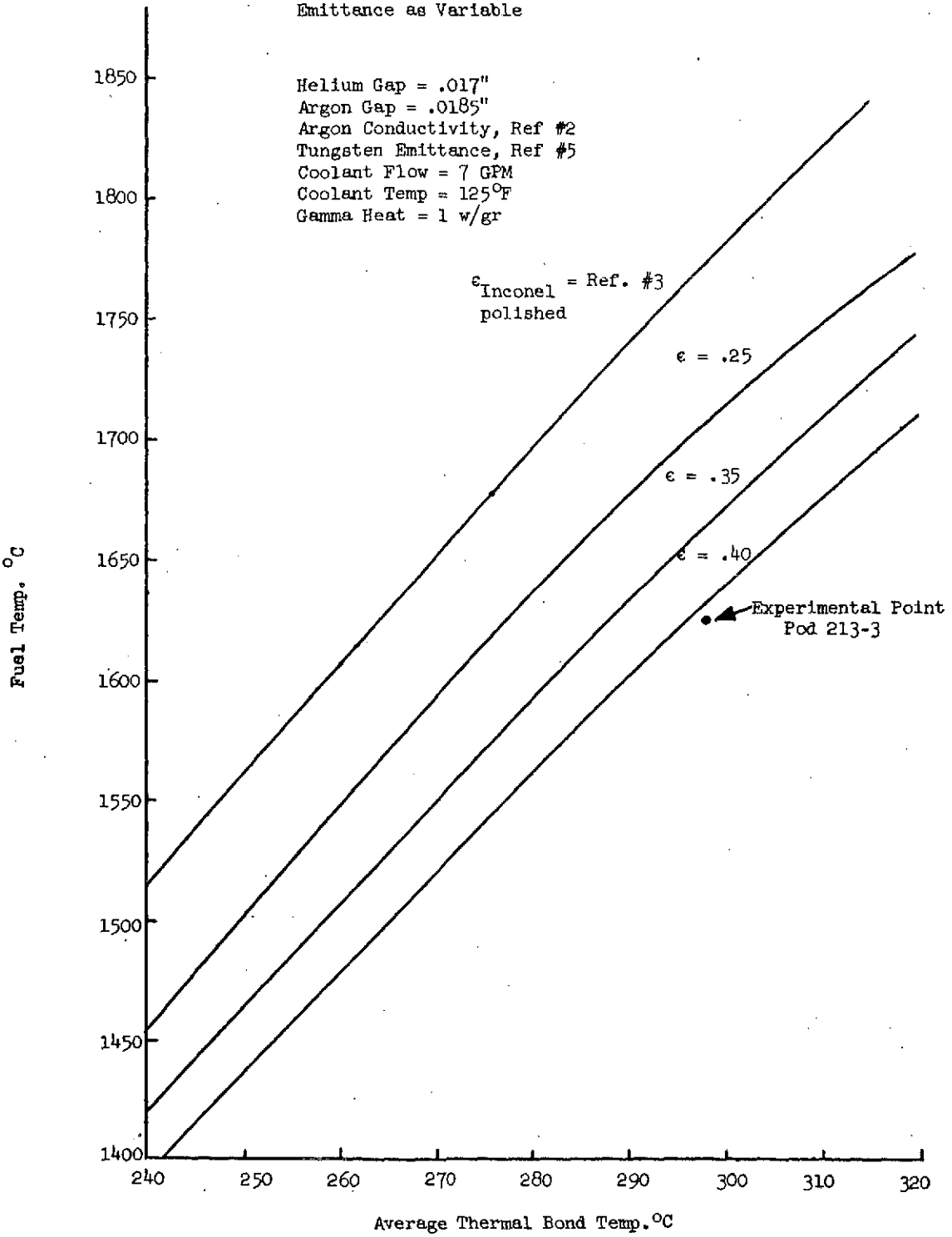

thermocouple reading versus the 295°C for the average low temperature thermocouple reading) does not represent a true fuel temperature versus thermal bond temperature relationship for the following reasons.

(1) During the startup, fuel pods 213-3 and 213-6 were located in regions of about equal neutron flux. Therefore the fuel temperature on pod 213-3 should be expected to be about the same as that in pod 213-6. The experimental results, however, indicated otherwise; the high temperature thermocouple in pod 213-3 read 1618°C while the high temperature thermocouple in pod 213-6 read 1730°C. Since thermocouples rarely read higher but can read lower than the true temperature because of an electrical shortage upstream from the hot junction, it is believed that the 1618°C reading rather than the 1730°C reading is in error.

(2) Compared with fuel pod 213-6 for which good correlation between experimental and calculated results was obtained, the γ heating rate has to be higher (1 w/gr. versus 0.75 w/gr.) and the fission power density has to be lower (350 w/cm^3 versus 450 w/cm^3) in fuel pod 213-3 in order to achieve good correlation. This is contradictory to the fact that in the V-2 region, the γ flux and the neutron flux show changes in a similar rather than opposite direction. (+33% change in γ heating rate accompanied by a -22% change in effective thermal neutron flux.)

(3) The high Inconel emittance required (0.40) for good correlation is inconsistent with the polished finish of the Inconel surface. It is doubtful that enough deposit could have been accumulated during the initial startup period to increase the emittance from 0.5 to 0.40.

Thus the above analysis indicates that a good correlation exists between the experimental and the calculated fuel temperatures versus average thermal bond temperature relationship during the initial startup for fuel pod 213-6, but not for fuel pod 213-3. The relationship established for

fuel pod 213-6 and the parametric curves of Fig. A.7 are used below to evaluate the fuel temperatures and the fission power densities in the four fuel pods as a function of irradiation time.

EVALUATION OF FUEL TEMPERATURES AND FISSION POWER DENSITIES IN IRRADIATED FUEL PODS AS A FUNCTION OF IRRADIATION TIME

The fuel temperatures and the fission power densities in the four irradiated fuel pods were deduced from their average thermal bond temperature history (Fig. A.2) by using the relationships shown in Fig. A.8 and Fig. A.9. The results obtained are shown in Figs. A.12 (a) and (b). Such deductions were made by assuming that the conditions prevailing in each fuel pod were the same as that specified in Fig. A.8 throughout the two irradiation cycles. Since this is not exactly true, the results shown in Figs. A.12 (a) and (b) are subjected to various degrees of uncertainties. These uncertainties are analyzed below for each fuel pod on the basis of the allowable variations in the values of the parameters involved, the parametric curves in Fig. A.7 and the guiding principle that at any time during the irradiation the γ heating rates and the neutron flux densities in these fuel pods can shift from the initial values in fuel pod 213-6 only in the same direction, i.e. both are bigger or both are smaller but not one is bigger and the other is smaller than the initial values in fuel pod 213-6.

(1) Fuel pod 213-6. The good agreement between the experimental and the calculated fuel temperature versus average thermal bond temperature relationship shown in Fig. A.8 indicates that the initial fuel temperatures and fission power densities shown in Fig. A.12 (a) should involve very little uncertainties. However, as the irradiation proceeds, it is expected that the major perturbation is the change of the γ heating rate and the neutron flux density, which alters the relationship among the thermal bond temperature, the fuel temperature and the fission power density, although the other parameters may remain essentially unchanged from those specified in condition I of Fig. A.7. Since the γ heating rate and the neutron flux density have to

Fig. A.12--Fuel Temperatures and Fission Power Densities in Fuel Pods as a Function of Irradiation Time

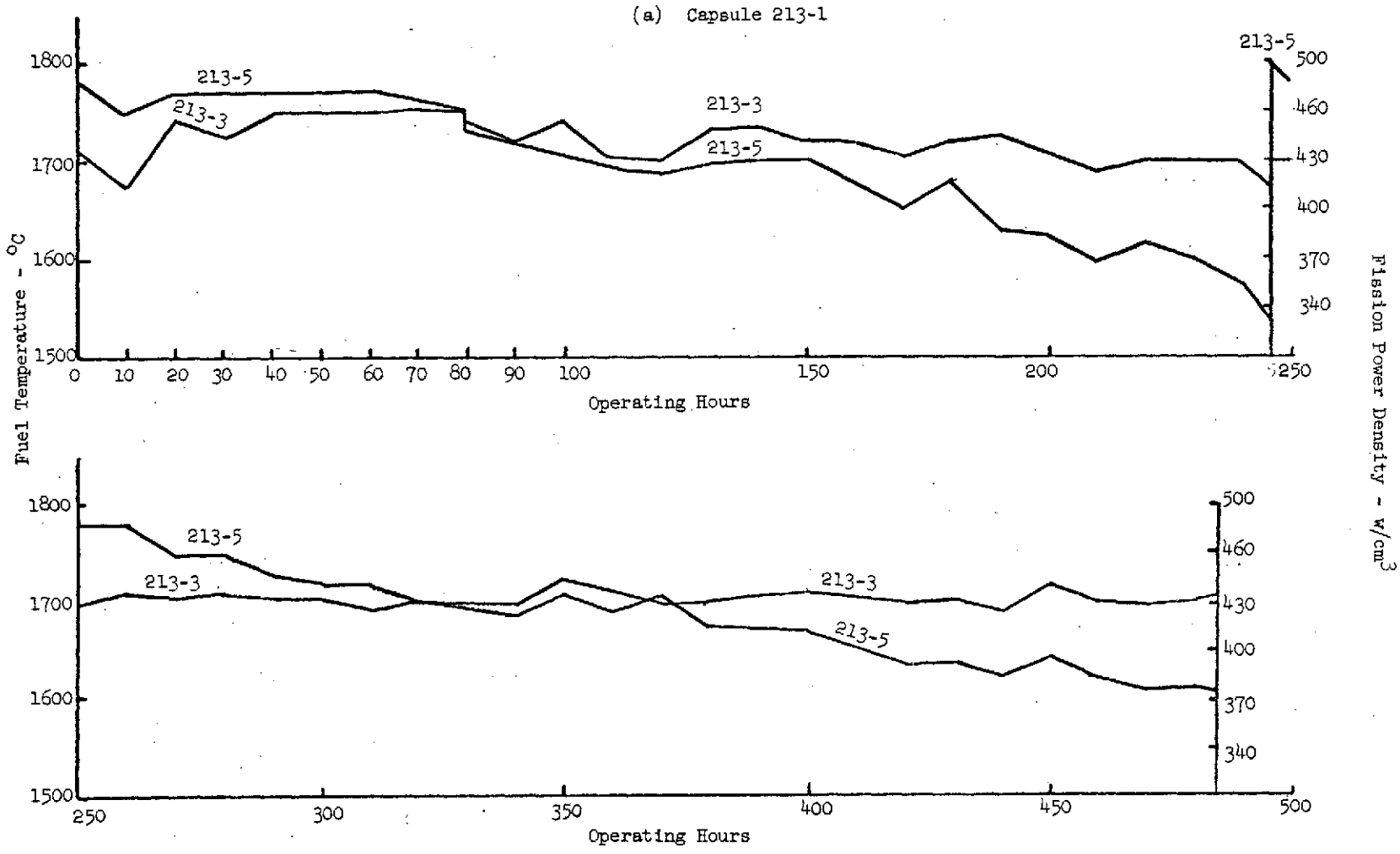

Fig. A.12--Fuel Temperatures and Fission Power Densities in Fuel Pods as a function of Irradiation Time (Continued).

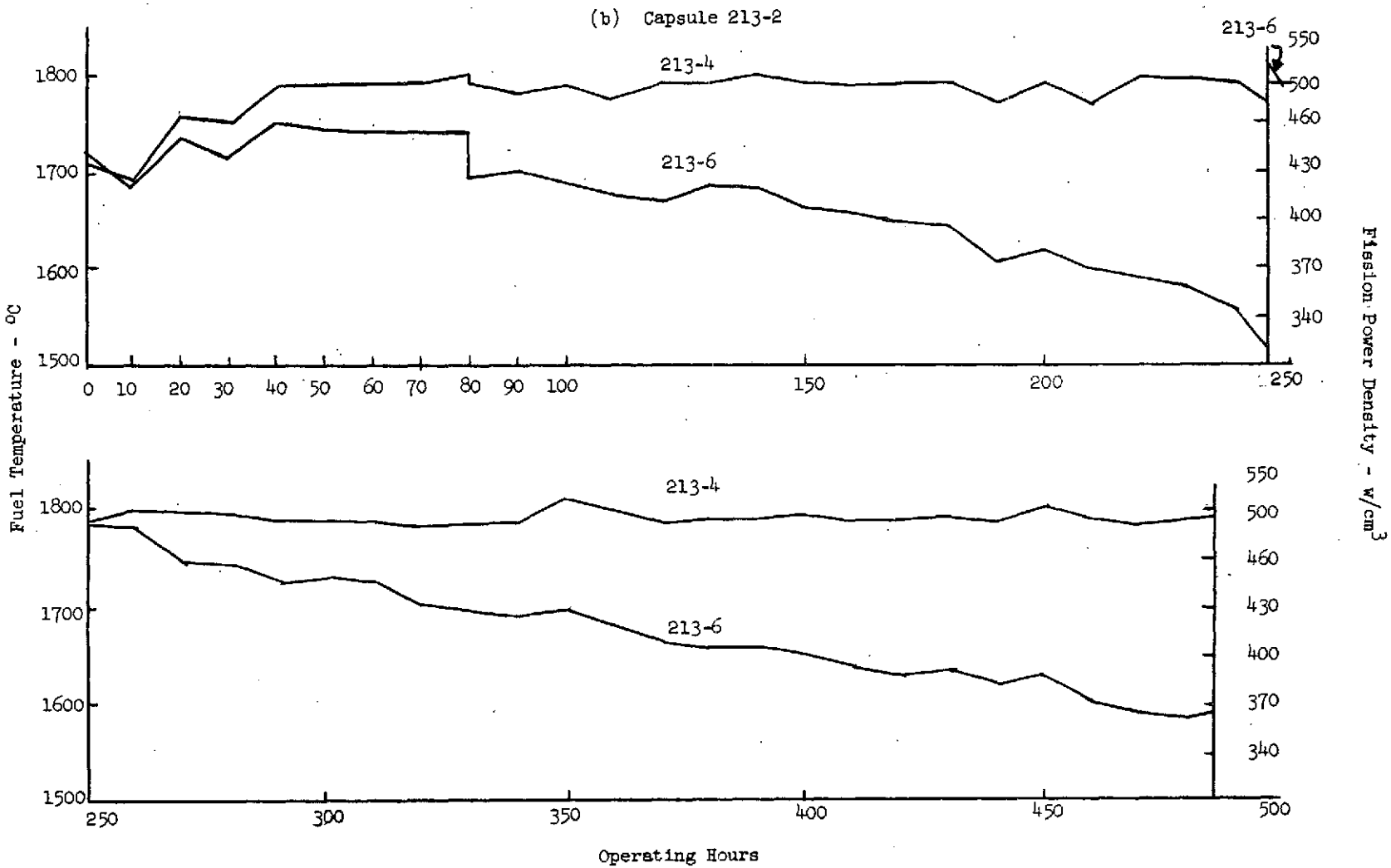

both increase or both decrease from the initial values in the fuel pod 213-6 (defined by point P in Fig. A.7), therefore for a given observed thermal bond temperature, the point defining the fuel temperature and the fission power density in Fig. A.7, when shifted from the original reference line A, can move only within certain areas. If the γ heating rate and the fission power density both become lower than the initial values defined by point P, then this area is bounded by the lines A, B and C to the left of point P. On the other hand, if both the γ heating rate and the fission power density become higher than the initial values defined by the point P, then this area is bounded by the lines A, C and D to the right of point P. The reason that line B and line D form the bounds of these areas is based on the assumption that the γ heating rate in the V-2 tube is limited to 0.5 - 1.0 w/gr. Since the data shown in Fig. A.3 indicate that the average thermal bond temperature for fuel pod 213-6 is less than $293^{\circ}C$ throughout the two irradiation cycles, it can be seen from Fig. A.7 that the maximum uncertainties in fuel temperature and fission power density are defined by the vertical distance between line A and line B, which amounts to $\sim 30^{\circ}C$ for the fuel temperature and ~ 30 w/cm^3 for the fission power density.

(2) Other fuel pods. For the other three fuel pods, the uncertainties in the fuel temperatures and fission power densities shown in Fig. A.12 are due to the differences in both the γ heating rate and the values of the other parameters from the reference values of line A shown in Fig. A.7. A similar analysis by invoking the same guiding principle described above but with operation possible in both condition I and condition II indicates that for the observed average thermal bond temperatures shown in Fig. A.3, the maximum uncertainties on fuel temperatures and fission power densities in these fuel pods are defined by the vertical distance between the reference line A and the line E. Below line E the γ heating rate increases but the fission power density

decreases, i.e. the guiding principle is not obeyed. These uncertainties amount to $\sim 120^{\circ}C$ for the fuel temperature and ~ 70 w/cm^3 for the fission power density.

CONCLUSIONS

The calculated fuel temperature and fission power density ranges during the two irradiation cycles are taken from Fig. A.12 and shown in Table A.III. The uncertainties in these ranges due to possible variations in dimensions and gamma heating rate are also indicated here.

It must be pointed out that in the above treatment, the Inconel emittance is assumed to be uniform from pod to pod and to remain constant during the two reactor cycles. While this is probably true during these two initial reactor cycles, as indicated by the similarity between the average thermal bond temperature history of these fuel pods during these two cycles, no projection can be made, without a very detailed supporting experiment, of the change in the fuel temperature-thermal bond temperature correlation with time due to possible Inconel emittance changes.

As shown in Fig. A.3, there is good agreement in thermal bond temperature between the two top fuel pods and between the two bottom fuel pods, which indicates that the neutron flux conditions in the two capsules are symmetrical with respect to the reactor core. The decrease in temperature of the two lower fuel pods with control rod withdrawal indicates that the axial location of the capsules in the V-2 tube is lower than optimum. It appears that an adjustment in location upward of 2-4 inches could reduce the temperature variation in the lower pods at the expense of a small temperature variation in the upper pods. This would give the smallest maximum and smallest average temperature variation for all spcimens.

TABLE A.III

Summary of Results

Fuel Pod Number		Fuel Temperature Range °C	Fission Power Density Range, w/cm^3	Uncertainties*	
				Fuel Temp., °C	Fission Power Density w/cm^3
Capsule	213-3	1675-1750	410-464	120	70
213-1	213-5	1540-1785	333-488	120	70
Capsule	213-4	1690-1815	418-510	120	70
213-2	213-6	1520-1810	329-507	30	30

*For fuel pod 213-6, the true fuel temperature and the true fission power density could be higher than the values shown on the table by a maximum of 30°C and 30 w/cm^3 respectively. For fuel pods 213-3, -4, and -5, the true fuel temperature and the true fission power density could be lower than the values shown in the table by a maximum of 120°C and 70 w/cm^3 respectively. These uncertainties are estimated on the basis of the following assumptions: (1) the γ heating rate and the fission power density have to shift in the same direction, (2) the parameters can vary only in the ranges specified in the text, and (3) the Inconel emittance did not change during the two cycle irradiation.

REFERENCES

1. Tsederberg, N. V., "Thermal Conductivity of Gases and Liquids," M.I.T. Press, 1965.

2. Keyes and Vines, "Thermal Conductivity of Nitrogen and Argon," Transaction of the ASME, Vol. P7, No. 2, May, 1965.

3. Goldsmith, Alexander, Handbook of Thermophysical Properties, Vol. II, The Macmillan Company, New York, 1961.

4. Thermal Radiation Properties of Selected Materials, DMIC Report No. 177, Vol. I, Nov. 1962.

5. Gubareff, G. G., Shao-Yen Ko., P. E. McNall, Jr., Review of the Thermal Radiation Property Values for Metals and Other Materials. Minneapolis-Honeywell Regulator Co. Report GR 2462-R3, September 1958 p. 139.

DISTRIBUTION LIST

National Aeronautics and Space Administration
Lewis Research Center
21000 Brookpark Road
Cleveland, Ohio 44135
Attn: John E. Dilley, MS500-309 (1)

National Aeronautics and Space Administration
Western Operations Office
150 Pico Boulevard
Santa Monica, California 90406
Attn: John Keeler (1)

National Aeronautics and Space Administration
Manned Spacecraft Center
Houston, Texas 77058
Attn: Bobby Bragg (1)

National Aeronautics and Space Administration
400 Maryland, S. W.
Washington, D. C. 20546
Attn: James J. Lynch, Code RNP (1)
Fred Schulman, Code RNP (1)

National Aeronautics and Space Administration
Lewis Research Center
2100 Brookpark Road
Cleveland, Ohio 44135
Attn: Roland Breitweiser, MS 302-1 (1)
Robert Migra, MS 49-2 (1)
James Ward, MS 500-201 (1)
Ralph Forman, MS 302-1 (1)

National Aeronautics and Space Administration
Lewis Research Center
21000 Brookpark Road
Cleveland, Ohio 44135
Attn: Roger Mather, MS 500-309 (1)
Herman Schwartz, MS 500-309 (1)
Report Control, MS 5-5 (1)
John J. Weber, MS 3-16 (1)
Robert Denington, MS 500-309 (1)
T. A. Moss, MS 500-309 (1)
H. B. Probst, MS 49-1 (1)
Library, MS 3-7 (1)

Neal Saunders, MS 105-1 (1)
John W. R. Creagh, MS 500-309 (3)
Bernard Lubarsky, MS 500-201 (1)
Vince Hlavin, MS 3-14 (1)

National Aeronautics and Space Administration
Ames Research Center
Moffett Field, California 94035
Attn: Library (1)

National Aeronautics and Space Administration
Goddard Space Flight Center
Greenbelt, Maryland 20771
Attn: Library (1)
Joseph Epstein (1)

National Aeronautics and Space Administration
Langley Research Center
Langley Field, Virginia 23365
Attn: Library (1)

Battelle Memorial Institute
505 King Ave.
Columbus, Ohio 43201
Attn: David Dingee (1)
Don Keller (1)

Battelle Memorial Institute
Pacific Northwest Laboratories
1112 Lee Boulevard
P. O. Box 999
Richland, Washington 99352
Attn: R. F. Dickerson (1)

The Boeing Company
P. O. Box 3707
Seattle, Washington
Attn: Grady Mitchan, MS 22-21 (1)

Bureau of Ships
Department of the Navy
Washington 25, D. C.
Attn: John Huth, Code 305 (1)
B. B. Rosenbaum, Code 342B (1)
E. P. Lewis, Code 1500 (1)

Douglas Aircraft Company
Missile and Space Engineering
Nuclear Research (A2-260)
3000 Ocean Park Blvd.
Santa Monica, California
Attn: A. DelGrossa (1)

Electro-Optical Systems, Inc.
300 North Halstead Avenue
Pasadena, California
Attn: A. Jensen (1)

Ford Instrument Company
32-36 47th Avenue
Long Island City, New York
Attn: Al Medica (1)

General Electric Company
Missile and Space Division
P. O. Box 8555
Philadelphia, Pennsylvania 19101
Attn: ANSE (1)

General Electric Company
Knolls Atomic Power Laboratory
Schnectady, New York
Attn: R. Ehrlich (1)

North American Aviation
S&ID Division
12214 Lakewood Boulevard
Downey, California
Attn: C. L. Gould (1)

Oak Ridge National Laboratory
Oak Ridge, Tennessee
Attn: Library (1)

Office of Naval Research
Power Branch
Department of the Navy
Washington, D. C. 20360
Attn: Cmdr. W. Diehl (1)

Pratt & Whitney Aircraft Corp.
East Hartford 8, Connecticut
Attn: William Lueckel (1)

Radiation Effects Information Center
Battelle Memorial Institute
505 King Avenue
Columbus, Ohio 43201
Attn: R. E. Bowman (1)

Radio Corporation of America
New Holland Ave.
Lancaster, Pennsylvania
Attn: Fred Black (1)

Radio Corporation of America
David Sarnoff Research Center
Princeton, New Jersey
Attn: Paul Rappaport (1)

The Rand Corporation
1700 Main Street
Santa Monica, California 90406
Attn: Ben Pinkel (1)

Republic Aviation Corporation
Farmingdale, L. I., New York
Attn: Alfred Schock (1)

General Electric Company
Electronic Components Division
One River Road
Schenectady, New York
Attn: Dr. D. A. Wilbur, Manager-Tube Research (1)

General Electric Company
Nuclear Materials & Propulsion Operation
P. O. Box 15132
Cincinnati, Ohio 45215
Attn: J. A. McGurty (1)
E. Delson (1)

General Electric Company
Research Laboratory
Schenectady, New York
Attn: Volney C. Wilson (1)

National Aeronautics and Space Administration
Marshall Space Flight Center
Huntsville, Alabama 35812
Attn: Library (1)
Edward Dungan (1)

NASA-Scientific and Technical Information Facility
P. O. Box 33
College Park, Maryland 20740 (2+ Repro)

Aerojet-General Nucleonics
San Ramon, California 94583
Attn: K. Johnson (1)

Aerospace Corporation
P. O. Box 95085
Los Angeles, California
Attn: Library (1)

Air Force Cambridge Research Laboratory
L. G. Hanscom Field
Bedford, Massachusetts 01730
Attn: CRZAP (1)

Air Force Weapons Laboratory
Kirtland Air Force Base
New Mexico 87117
Attn: Library (1)
Lt. Donald A. Brooks (WLDA-3) (1)

Flight Vehicle Power Branch
Air Force Aero Propulsion Laboratory
Wright-Patterson Air Force Base, Ohio 45433
Attn: A. E. Wallis (1)

Space Systems Division (SSTRE)
AF Unit Post Office
Los Angeles, California 90045
Attn: Major W. Iller (1)

Allison Division
General Motors Corporation
Indianapolis, Indiana 46206
Attn: T. L. Rosebrock (1)

Argonne National Laboratory
9700 South Cass Avenue
Argonne, Illinois 60439
Attn: Aaron J. Ulrich (1)

Atomis International
P. O. Box 309
Canoga Park, California 91304
Attn: Robert C. Allen (1)
Charles K. Smith (1)

Babcock & Wilcox Comapny
1201 Kemper Street
Lynchburg, Virginia 24505
Attn: Frank R. Ward (1)

General Electric Company
Atomic Power Equipment Department
P. O. Box 1131
San Jose, California 95108
Attn: Alleen Thompson
For: Don Francis (1)
B. G. Voorhees (1)
J. VanHoomissen (1)

General Motors Corporation
Research Laboratories
12 Mile & Mound Roads
Warren, Michigan
Attn: F. E. Jamerson (1)

Institute for Defense Analysis
1666 Connecticut Avenue, N. W.
Washington 9, D. C.
Attn: R. C. Hamilton (1)

Jet Propulsion Laboratory
California Institute of Technology
4800 Oak Grove Drive
Pasadena, California 91103
Attn: Peter Rouklove (1)
Gerry Davis (1)

Los Alamos Scientific Laboratory
P. O. Box 1663
Los Alamos, New Mexico 87544
Attn: G. M. Grover (1)
E. Salmi (1)

Marquardt Corporation
Astro Division
16555 Saticoy Street
Van Nuys, California 91409
Attn: A. N. Thomas (1)

Martin-Nuclear Division of Martin-Marietta Corp.
P. O. Box 5043
Middle River, Maryland 21220
Attn: W. J. Levedahl (1)

Lockheed Missiles & Space Division
Mr. Charles A. Putney
P. O. Box 141
Sunnyvale, California 94086
Attn: H. H. Greenfield (1)

TRW Space Technology Laboratories
One Space Park
Redondo Beach, California 92078
(Attn: Margaret N. Sloane, Chief Librarian) (1)

Texas Instruments, Inc.
P. O. Box 5474
Dallas 22, Texas
Attn: R. A. Chapman (1)

U. S. Army Erdl
Fort Monmouth, New Jersey 07703
Attn: Emil Kittil (1)

U. S. Atomic Energy Commission
Germantown, Maryland
Attn: Cmdr. Morris Prosser (1)

U. S. Atomic Energy Commission
Technical Reports Library
Washington 25, D. C.
Attn: J. M. O'Leary (3)

U. S. Atomic Energy Commission
Div. of Technical Information
Extension
P. O. Box 62
Oak Ridge, Tennessee 37831 (3)

U. S. Atomic Energy Commission
San Francisco Operations Office
2111 Bancroft Way
Berkeley California 94704
Attn: Don Beard (1)

Varian Associates
611 Hansen Way
Palo Alto, California
Attn: Ira Weismann (1)

Westinghouse Electrical Corp.
Astronuclear Lab
P. O. Box 10864
Pittsburgh, Pennsylvania 15236 (1)

Thermo Electron Engineering Corp.
Security Officer
P. O. Box 482
Waltham, Massachusetts 02154

Mark inside envelope (classified only)
Thermo Electron Engineering Corp.
85 First Ave.
Waltham, Massachusetts 02154
Attn: George Hatsopoulos (1)
Robert Howard (1)

Dr. James Hadley
Head, Reactor Division
Lawrence Radiation Laboratory
Livermore, California 94551 (1)

Astro Met Associates, Inc.
500 Glendale-Milford Road
Cincinnati 15, Ohio
Attn: John W. Graham (1)

Bendix Corporation
696 Hart Avenue
Detroit, Michigan (1)

University of Arizona
Tucson, Arizona
Attn: Monte V. Davis (1)